Inhibition of Carbonic Anhydrase IX in Glioblastoma Multiforme

by

Abdolali Amiri

Department of Pharmacology and Therapeutics

Faculty of Medicine

McGill University, Montreal

August 2015

A thesis submitted to McGill University in partial fulfillment of the requirements of the degree of Master of Science (MSc)

Dedicated to

My parents,

for their constant encouragement and support

and

My brother,

whose limitless strength and positivity always inspires me

Table of Contents

Acknowledgments

I would like to express my most sincere gratitude to my supervisor, **Dr. Dusica Maysinger**, for her constant help, support and encouragement. Thank you for generating a stimulating environment in the lab and keeping your door always open and welcoming at any time.

My thesis committee and my advisor provided invaluable support and feedback. A special thank you goes to **Dr. Guillermina Almazan**, **Dr.Tak Pan Wong** and **Dr. Terry Hebert**. A very special thank you goes to **Dr. John Gillard** for his helpful tips and insights and constant support throughout my entire experience as a graduate student. Dr. Nathan Yoganathan was an essential collaborator and provided me with the antibody needed to carry out the studies.

Lab members and colleagues, past and current, made the journey an enjoyable experience and helped through their guidance, suggestions, and technical assistance. Thank you: **Diana Mejia**, **Sebastien Boridy**, **Angela Choi**, **David Cui**, **Eliza Hutter**, **Jeff Ji**, **Alex Moquin**, **Kevin Neibert**, **Wolfgang Reintsch**, **and Issan Zhang**. Finally, I would like to thank the staff members who make the department a positive environment for all the students: **Hélène Duplessis**, **David Kalant**, **Chantal Grignon** and **Tina Tremblay**.

Abstract

Background: Glioblastoma multiforme (GBM) is the most common and most aggressive malignant primary brain tumor in humans. Median survival with standard-of-care radiation and chemotherapy with temozolomide (TMZ) is 15 months. Median survival without treatment is 4 1/2 months. The treatment of GBMs remains difficult in that no contemporary treatments are curative. In addition, brain tumor stem cells (BTSC), the tumorigenic cells, are postulated to be responsible for recurrence of GBM and may be the main cause of therapeutic failure when targeting GBM with TMZ, which induces apoptosis and necroptosis-based cell death.

One way to improve the effectiveness of the current therapies is to use combination of drugs with sensitizers. Tumor cores, including those of GBM, are hypoxic, which is a condition commonly associated with poor responses to chemotherapies. In addition, GBM has a highly glycolytic energy cycle, leading to hyper acidification of the tumour cytoplasm. Recent studies have shown that a carbonic anhydrase (CA) isoform, CA IX, is selectively overexpressed by tumor cells, especially GBM, and shows highly restricted expression in normal tissue. A most exciting recent finding also implicates CA IX in the maintenance of a (breast) cancer stem-cell phenotype. CA IX has a dual role in the growth of hypoxic, CO_2 excreting tumors. First, it helps to produce and maintain an internal alkaline pH favorable for tumor growth. Second, it promotes tumor cell invasiveness by stromal acidification. Moreover, the acidification of the extracellular milieu is unfavourable to the obligatory chemical activation of the only current treatment for GBM, TMZ. **Hypothesis and main objectives:** We hypothesize that inhibition of CA IX by acetazolamide (ATZ, a broad-spectrum CA inhibitor used in clinical treatment of altitude sickness) and an anti-CA IX antibody (provided by an industrial sponsor) will enhance the effectiveness of TMZ in GBM 2D and 3D cell models. **Results**: CA IX expression was significantly increased by $CoCl_2$ (dose dependent) and the highest cell death was caused by ATZ/TMZ combination after 6 days under hypoxia in U251N monolayers ($p<0.01$). In spheroids (U251N) CA IX expression was time and size dependent. We demonstrated a presence of CA IX in BTSC in culture. ATZ caused minimal cell death. Combination with TMZ in spheroids caused the most significant cell

death after 6 days ($P<0.0001$) with correlative expression of BAX ($p<0.05$). Caspase-3 activity was increased most significantly for ATZ/TMZ combination in both 2D and 3D cultures ($p<0.0001$ and $p<0.05$ respectively). The encapsulation of ATZ into micelles significantly increased cell death in spheroids at all the time points (1-6 days), alone and in combination with TMZ. All data are representative of at least 2 to 6 independent experiments. **Significance:** TMZ has a poor *in-vitro* activity, but it is the only current drug to treat GBM. CA IX inhibition appears to influence cell survival alone and makes cells more sensitive to TMZ. A significant cell death induced in GBM and BTSC by micellar ATZ is an exciting finding which will permit *in-vivo* evaluations using tumours generated from patient-derived GBM stem cells.

Résumé

Contexte: Le glioblastome multiforme (GBM) est la plus fréquente et la plus agressive des tumeurs primaires malignes du cerveau chez l'homme. La médiane de survie suite à des soins standards de radiations et de chimiothérapie par le témozolomide (TMZ) est de 15 mois. La médiane de survie sans traitement est de 4 mois et demi. Le traitement des glioblastomes reste difficile étant donné qu'aucun des traitements actuels ne sont curatifs. De plus, les cellules souches de tumeur cérébrale (BTSC), les cellules tumorigènes, sont supposées être responsables de récidive du glioblastome et peuvent être la principale cause d'échec thérapeutique en ciblant le glioblastome avec le TMZ, qui induit l'apoptose et la mort cellulaire par nécroptose. Une façon d'améliorer l'efficacité des thérapies actuelles est d'utiliser une combinaison de médicaments avec des sensibilisateurs. Le centre des tumeurs, y compris ceux du glioblastome, sont hypoxiques, qui est une condition souvent associée à peu de réponses aux chimiothérapies. De plus, le glioblastome a un cycle glycolytique hautement énergétique, conduisant à une hyper acidification du cytoplasme de la tumeur. Des études récentes ont montré que l'isoforme de l'anhydrase carbonique (CA), CA IX, est sélectivement surexprimé par les cellules tumorales, en particulier le glioblastome, et est très restrictivement exprimé dans les tissus normaux. Une excitante et récente découverte implique également CA IX dans le maintien du phénotype des cellules souches du cancer du sein. CA IX a un double rôle dans la croissance des tumeurs hypoxiques, excrétant de CO_2. Premièrement, il est important de produire et de maintenir un pH alcalin interne favorable à la croissance de la tumeur. Deuxièmement, il favorise la capacité d'invasion de la cellule tumorale est favorisée par une acidification stromale. De plus, l'acidification du milieu extracellulaire est défavorable à l'obligatoire activation chimique du seul traitement en cours pour les GBM, le TMZ. **Hypothèses et Objectifs principaux** : Notre hypothèse est que l'inhibition de CA IX par l'acétazolamide (ATZ, un inhibiteur de l'anhydrase carbonique à large spectre utilisé dans le traitement clinique du maladies d'altitude) et un anticorps anti-CA IX (fournie par un partenaire industriel) permettra d'améliorer l'efficacité du TMZ dans des modèles cellulaires 2D et 3D de glioblastome. **Résultats**: L'expression de CA IX a été

significativement augmentée par le $CoCl_2$ (dose dépendant) et la plus forte mort cellulaire a été causée par une combinaison d'ATZ/TMZ après 6 jours en hypoxie dans des monocouches d'U251N ($p < 0,01$). Dans les sphéroïdes (U251N), l'expression de CA IX est dépendant du temps et de la taille. Nous avons démontré la présence de CA IX dans les BTSC en culture. L'ATZ a causé une mort cellulaire minime. La combinaison avec le TMZ dans les sphéroïdes a causé la plus significative mort cellulaire après 6 jours ($p< 0,0001$), corrélée avec une expression de BAX ($p< 0,05$). L'augmentation la plus significative de l'activité caspase-3 a été détecté pour la combinaison ATZ/TMZ dans les cultures 2D et 3D ($p < 0,0001$ et $p < 0,05$ respectivement). L'encapsulation de l'ATZ dans les micelles a significativement augmentée la mort cellulaire dans les sphéroïdes à toutes les différentes mesures de temps (1-6 jours), en monothérapie ou en combinaison avec TMZ. Toutes ces données sont représentatives d'au moins 2 à 6 expériences indépendantes. **Conclusion**: Le TMZ a une faible activité *in vitro*, mais il est le seul médicament actuel pour traiter le glioblastome. L'inhibition de CA IX semble influencer la survie cellulaire et rend les cellules plus sensibles au TMZ. Une mort cellulaire significative induite dans le GBM et BTSC par l'ATZ micellaire est une découverte intéressante qui permettra des évaluations *in vivo* utilisant des tumeurs générées à partir de cellules souches de glioblastome provenant de patients.

List of Tables

List of Figures

List of Abbreviations

API, Active pharmaceutical ingredient

ATZ, Acetazolamide

BBB, Blood brain barrier

BTSC, brain tumor stem cells

CA, carbonic anhydrase

CIMP, Cytosine phosphate guanine island methylation phenotype

CNS, Central nervous system

CpG, Cytosine phosphate guanine

DLS, Dynamic light scattering detector

DMEM, Dulbecco's Modified Eagle Medium

DWF, Differential weight fraction

EGFR, Epidermal growth factor receptor

EMT, Epithelial-mesenchymal transition

FBS, Fetal bovine serum

FDA, Food and Drug Administration

FISH, Fluorescent in situ hybridization

FTI, Farnesyltransferase

GBM, Glioblastoma multiforme

GEMM, Genetically engineered mouse model

HDAC, Histone deacetylase

HGG, High grade glioma

hGSC, Human glioblastoma stem cell

HIF, Hypoxia inducible factor

HSP90, Heat-shock protein 90

IDH, isocitrate dehydrogenase

IHC, Immunohistochemistry

m/unm, methylated/unmethylated

MGMT, O6–methguanine-DNA methyltransferase

MRI, magnetic resonance imaging

MTIC, (5-(3-Methyltriazen-1-yl) imidazole-4-carboximide)

OA, Oligoastrocytoma

OS, Overall survival

PARP, Poly (ADP-ribose) polymerase

PBS, Phosphate buffer solution

PDGFR, Platelet-derived growth factor receptor

PEG-PLGA, Poly-(ethylene glycol) methyl ether-block-poly-(lactide-co-glycolide)

PI, Propidium Iodide

PI3K, Phosphatidylinositol 3-kinase

RT, Radiotherapy

RT, Room temperature

SEM, Standard error of the mean

TGF-β, Tumor growth factor-β

THF, tetrahydrofuran

TMZ, temozolomide, v

WHO, World Health Organization

WT, Wild type

Contribution of Authors

Part of the work presented herein was made possible by collaboration with the following colleagues:

Dr. Nathan Yoganathan has supervised synthesis, design and characterizations of anti-CA IX antibody used for biological experiments.

Dr. Phuong Uyen Le isolated human glioblastoma stem cells and has done the XTT assays on the BTSCs.

Dr. Alexandre Moquin synthesized the ATZ micelles described in materials and method.

The author has performed all biological experiments under the supervision of Dr. Dusica Maysinger and suggestions from Dr. John Gillard.

Manuscripts

CA IX inhibition in Glioblastoma Multiforme.

Abdolali Amiri, Phuong Uyen Le, Kevin Petrecca, John Gillard, Nathan Yoganathan, Dusica Maysinger

Manuscript in progress

Dimerization-based biosensor to reveal the responsiveness of glioblastoma cells and stem cells to chemotherapeutics.

Issan Zhang, Yiming Cui, Abdolali Amiri, Yidan Ding, Phuong Uyen Le, Kevin Petrecca, Robert E. Campbell, and Dusica Maysinger

Journal of Biology and Chemistry.

Manuscript submitted

Rationale and Objectives

CA IX is transmembrane enzyme induced by hypoxia in cancer cells where it plays several roles: (1) it helps to produce and maintain an internal alkaline pH, favourable for tumor survival and growth. (2) It promotes tumor cell invasiveness by dramatically facilitating the activity of extracellular proteases and diminishing immune responses directed at the tumour by exporting the acidity to the stroma. (3) It promotes motility and invasion of glioblastoma multiforme (GBM), possibly through a signalling mechanism independent of its catalytic function. Inhibition of CA IX interferes with removal of protons and results in a decrease in intracellular pH, negatively affecting cell survival. These factors indicate that CA IX is a potential metabolic target in GBM. We wish to expand our basic knowledge of sensitization to chemotherapy by CA IX inhibition.

The main objective of this study is to develop and characterize models of GBM to investigate the expression of CA IX and evaluate the responsiveness of GBM cells in culture to inhibitors of CA IX, individually and in combination with the first-line therapeutic anticancer agent, TMZ. The studies in this thesis also reveal the expression of CA IX in brain tumor stem cells (BTSC) derived from cancer patients and their responsiveness to CA IX inhibition and TMZ treatment.

One of the main limitations of anticancer therapy is limited access to the brain tumors. To overcome this limitation we propose to use micelles as a novel way for ATZ delivery to GBM. The effects of micelles with or without ATZ will be tested in U251N and BTSC spheroid cultures.

Chapter 1: Literature Review

1.1. Etiology and epidemiology of glioblastoma multiforme

Gliomas are primary brain tumors which are most commonly occurring in adults. The majority of gliomas are astrocytic (82%) while unspecified gliomas (7%), oligodentroglial tumors (6%), and mixed oligoastrocytomas (3%) form the rest (Dolecek, Propp, Stroup, & Kruchko, 2012). These divisions are based on histopathologic appearances, though, they consist of heterogeneous group of tumors. As they all have distinct molecular oncology and biology, some of them are classified according to the prognostic and predictive biomarkers

The 2007 World Health Organization has established classification for gliomas based on their histological and pathological observations. There are four grades of gliomas according, but not limited to, their invasiveness, necrosis and mitotic activities (Louis et al., 2007): Grade I or *pilocytic astromas*, grade II (low grade), grade III (anaplastic) and grade IV (glioblastoma, GBM). Grade I are defined as slow growing non-malignant tumors which affect children. When resected, they rarely progress into malignant phenotypes and are associated with long term survival (Bralten & French, 2011). Grade II tumors, *diffuse astromas*, are identified as slow growing tumors accompanied by the signs of proliferative activity and infiltration into surrounding brain, making complete surgical resection challenging. *Diffuse astromas* can be presented as benign or malignant while in 70% of the cases, they are capable of progressing to higher grades astromas (Maher et al., 2001). Grade III astromas, *anaplastic astromas*, are highly aggressive in young adults. Despite the treatments, *anaplastic astromas* have a tendency to recur or progress to grade IV glioblastoma within several years of diagnosis. However, these tumors are rare yet heterogeneous, and their diffusive nature makes them not amenable to total resection (DeAngelis, 2009). Grade IV astromas, *glioblastoma multiforme* (GBM), are the most common, aggressive, and malignant type of gliomas. GBM is also often resistant to therapeutic interventions because of the cell heterogeneity. In addition they have regions of pseudopalisading necrosis and microvascular proliferation. They have variety of genetic alterations affecting many

signalling pathways downstream of tyrosine kinase receptors such as epidermal growth factor receptor (EGFR), or affecting cell-cycle arrest pathways by p53 mutations (Holland, 2000). The mean survival of GBM patients is from 2 or 3 months to a maximum of a 1.6 years in spite of complete surgical removal in combination with radiotherapy and chemotherapy.

1.2. Biomarkers of glioblastoma

There are no reliable and easily detectable unique biomarkers for GBMs. Malignant tumors are typically characterized by molecular analysis of several tumor biomarkers which were also found in some other tumors. The two recognized classes of biomarkers in oncology are prognostic and predictive. The flow diagram indicating the stages of patient grouping starting from imaging using magnetic resonance (MRI) to biomarker analysis in suspected GBM is illustrated in Figure 1.

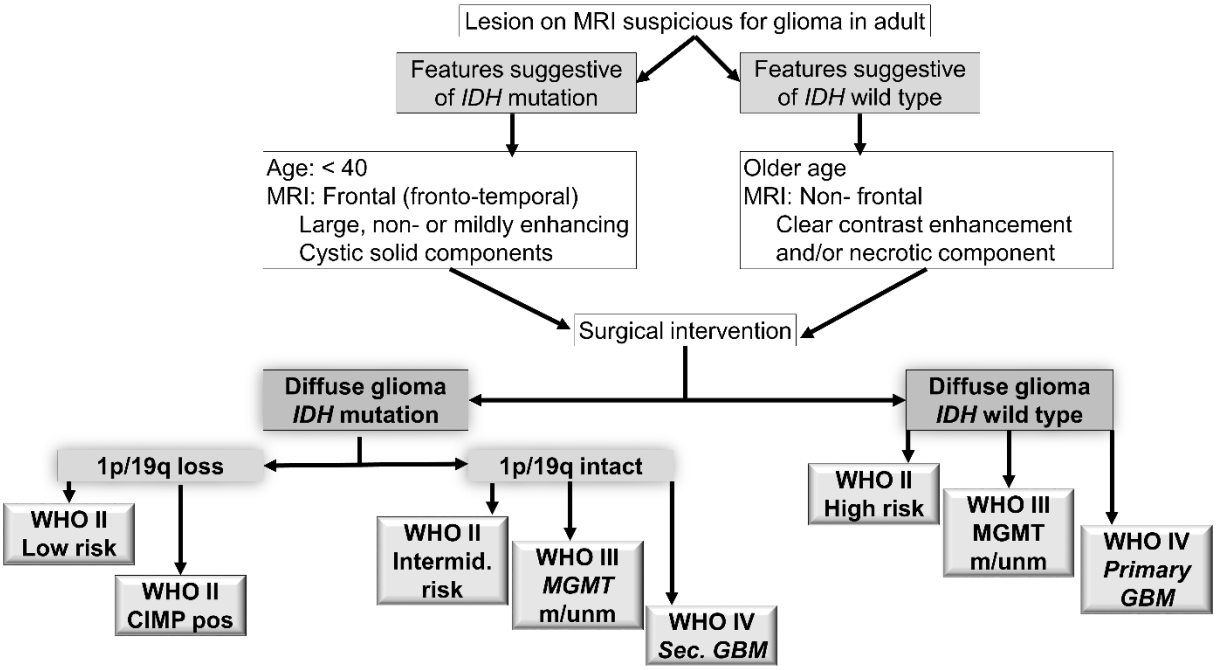

Figure 1. Clinical characteristics, histological and molecular classifications of adult gliomas.

CIMP = cytosine phosphate guanine (CpG) island methylation phenotype, GBM = glioblastoma multiforme, IDH = isocitrate dehydrogenase, intermed = intermediate, MGMT = O6–methguanine-DNA methyltransferase, m/unm = methylated/unmethylated, pos = positive, Sec. = secondary, WHO = World Health Organization. Adapted from (Siegal, 2015b) with permission from Elsevier.

Biomarkers shown in **Figure 1** are used as prognostic biomarkers which provide information about likely disease outcomes regardless of the treatment received. Predictive biomarkers inform about the expected outcomes depending on the applied interventions. There are three routinely assessed clinically relevant biomarkers used for diagnostic, prognostic and predictive purposes: ; isocitrate dehydrogenase 1 and 2 (IDH1/2) mutations, 1p and 19q chromosomal co-deletions and O^6–methguanine-DNA methyltransferase (MGMT) promoter methylation (Siegal, 2015a).

Clinical importance	**Molecular biomarkers**		
	IDH1/2 mutations	1p/19q	*MGMT* promoter methylation
	Frequency (%)		
Pilocytic astrocytoma	0	0	<10
Diffuse astrocytoma	70-80	15	40-50
Oligo/Oligoastrocytoma	70-80	30-60	60-80
Anaplastic atrocytoma	50-70	15	50
Anaplastic oligo/OA	50-70	50-80	70
GBM	5-10	<5	35
Biological implications	Linked to DNA and histone methylation, energy and metabolism	Unclear biological role, linked to oligo morphology	Silencing and impairment of DNA damage repair

Diagnostics implications	Differential diagnosis between diffuse glioma and gliosis	Oligo lineage	None
Prognostic marker	Yes- all histologies favorable	Yes- for oligo favorable	Yes astrocytice HGG favorable
Predictive marker	Yes- in AO with 1p/19q detection for chemoTX response	Yes-in AO with *IDH* mutation for chemoTx response	Yes- in anaplastic gliomas *IDH*-wt; GBM ≥ 70 years old

Table 1. Molecular biomarkers and their clinical relevance.
GBM = glioblastoma multiforme, HGG = high grade glioma, IDH = isocitrate dehydrogenase, MGMT = O6–methguanine-DNA methyltransferase, Oligo = oligodendroglioma, OA = oligoastrocytoma, Tx = therapy, wt = wild type. Adapted from (Siegal, 2015b) with permission from Elsevier.

Isocitrate dehydrogenase (IDH) is a catalytic enzyme which has at least three isoforms (IDH1,2 and 3). IDH 1 and 2 (IDH1/2) bear mutations, 1p and 19q chromosomal co-deletions and O^6–methguanine-DNA methyltransferase (MGMT) promoter methylation (Siegal, 2015a).

IDH3 mutations have not been observed in gliomas and IDH1 is the most common mutation. IDH1 is located in cytoplasm catalyzing the oxidative decarboxylation of isocitrate into alpha-ketoglutarate and NADPH. The mutated IDH1 converts isocitrate to 2-hydoxyglutarate instead leading to the significant accumulation of 2-HG gliomas (Dang et al., 2010). Gliomas are separated into *IDH*-wild-type and *IDH*-mutant tumors. While the *IDH*-mutations are mostly seen in younger patients, they are very rare in the elderly population (Hartmann et al., 2009; Korshunov et al., 2015). Several different

methods are adapted for diagnostic assessment of *IDH* status including the immunohistochemistry (IHC) and magnetic resonance spectroscopy.

1p and 19q chromosomal deletions have been typically associated with oligodendroglial tumors. However, the loss of 1p or 19q alone is sometimes seen in astromas but it is as strong prognostic implication as the co-deletion of 1p/19q in oligodendrogliomas (Reifenberger et al., 1994). One of the most frequent approaches to assess the 1p/19q deletion is the fluorescent *in situ* hybridization (FISH)(Nikiforova & Hamilton, 2011). The principle of FISH assay is illustrated in **Figure 2**.

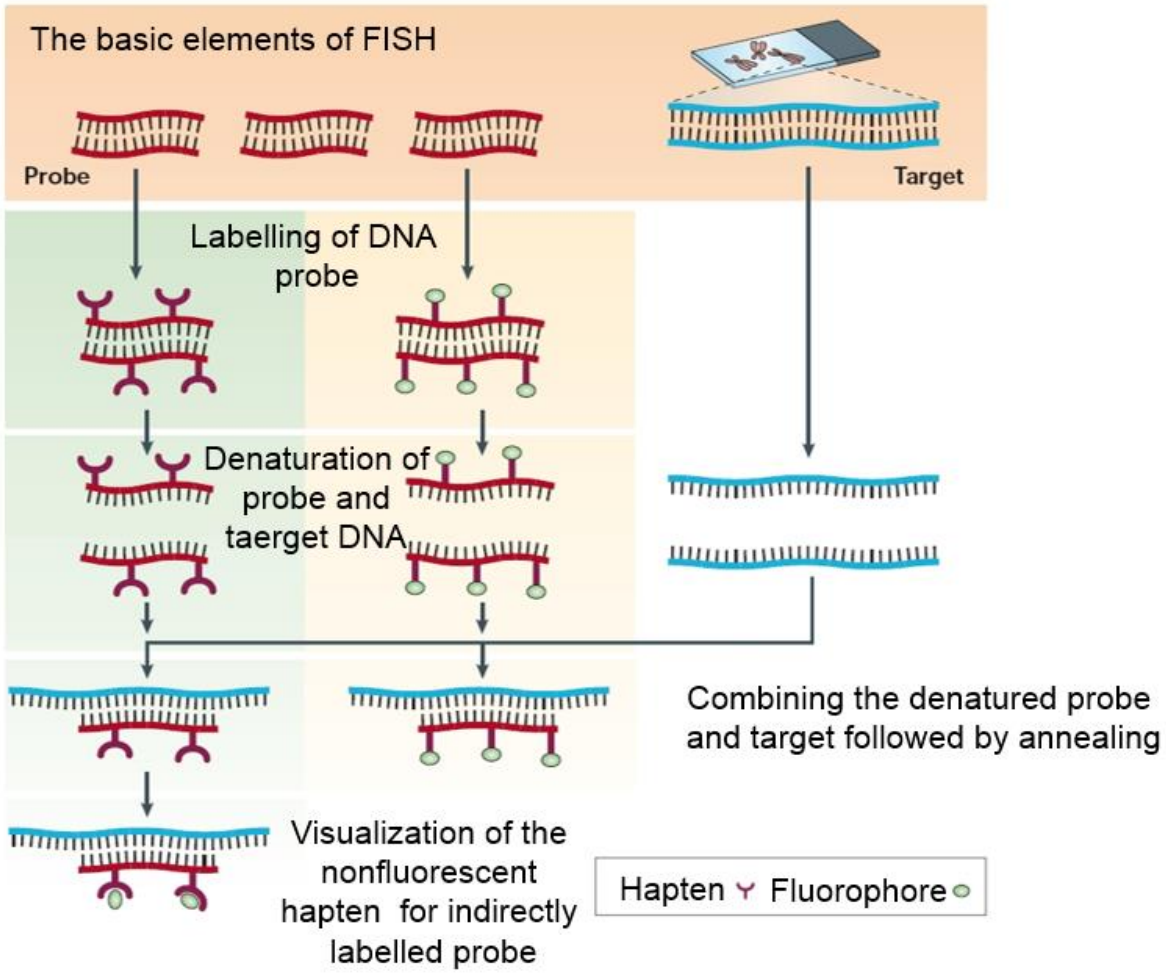

Figure 2. Schematic diagram of the fluorescence in situ hybridization (FISH) technique.

Adopted from (Speicher & Carter, 2005) with permission from Elsevier.

The MGMT gene located at 10q26 gene is ubiquitously expressed as a DNA repair enzyme that removes the alkyl adducts from guanine at O^6 position. DNA methylation, the covalent addition of a methyl group to cytosine or guanine nucleotide DNA methyl-transferases, is found on MGMT promoter in 35-45% of the high grade gliomas and in about 80% of low grade gliomas (Cankovic et al., 2013; Hegi et al., 2005). In addition, the primary tumor location seems to differ for methylated or unmethylated GBMs (Ellingson et al., 2012). Most studies have failed to prove MGMT methylation as a predictive of sensitivity to chemotherapy with temozolomide (TMZ), an alkylating agent commonly used for GBM in clinics. However, the analyses of several trials on elderly patients with high grade gliomas showed better outcome for chemotherapy with TMZ in patient with MGMT promoter methylation and lower survival for patients with unmethylated MGMT promoter (Malmstrom et al., 2012). Routinely, the MGMT methylation status is determined by extracting the tumor DNA from pathological specimen. Alternatively, free circulating DNA in serum or plasma of glioma patients is used for MGMT methylation status evaluation (Fiano et al., 2014; Lavon, Refael, Zelikovitch, Shalom, & Siegal, 2010).

1.3. Glioblastoma microenvironment: macrophages and peripheral myeloid cells

Under physiological conditions, CNS has a very close connection with the immune system (Casano & Peri, 2015). The infiltrating macrophages and the resident microglia, as immune cells, are hosted by the CNS under physiological conditions which are also abundantly present under pathological conditions. Macrophages are originated from mononuclear hematopoietic phagocytes which can infiltrate tissues and reorganize stress signals, clear debris and release combination of cytokine and chemokines (Perry & Gordon, 1988). Microglia, on the other hand, form a distinct population of macrophages in the CNS which are long lived and not normally replaced by peripheral cells. The accumulation of a huge number of immune cells i.e. microglia and macrophages (tumor associated myeloid cells) in the tumor mass is a remarkable feature of all gliomas especially in the high grade gliomas such as GBM (Badie & Schartner, 2000; Penfield, 1925). Macrophages derived from peripheral blood

accumulate in GBM when the blood brain barrier (BBB) is broken down while they are essentially restricted to the perivascular areas, meninx and choroid plexus in the brain free of tumor (Ransohoff & Engelhardt, 2012). Besides, In the tumor-free CNS, 5-10% of all brain cells (depending on the region) consists of microglia while under pathological conditions the number of tumor associated myeloid cells can reach up to 30% of the tumor mass in GBM (Badie & Schartner, 2001; Roggendorf, Strupp, & Paulus, 1996; Watters, Schartner, & Badie, 2005).

It has been over 90 years from the initial description of the abundant tumor-associated myeloid cells in the high grade gliomas. After several decades of research on the delineation of inefficient immune response, the conclusion was that it is the secretion of tumor growth factor-β (TGF-β) from the glioma cells that prevent induction of a coordinated response against the tumor (Kaminska, Kocyk, & Kijewska, 2013). This conclusion is in agreement with what is now evident about TGF-β signalling being vital for microglia under neuropathological conditions (Butovsky et al., 2014). The abundant expression and release of TGF-β was initially associated with tumor cells while now it is established that TGF-β can be generated from myeloid cells mediating important pathological effects (Kaminska et al., 2013; Wick, Naumann, & Weller, 2006; Yi et al., 2011).

Overall, the tumor associated myeloid cells seem to have the capacity to elicit both pro- and antitumor effect (Galarneau, Villeneuve, Gowing, Julien, & Vallieres, 2007; Sarkar et al., 2013). Thus it is of high interest to dissect the function of intratumoral macrophages or microglia to establish targets which are specific to the cell type for adjuvant therapies for gliomas.

1.4. The role of brain tumor stem cells in glioblastoma

The heterogeneous nature of tumor biology and the failure of currently available therapies give rise to a debate that revolves around BTSC as critical contributors to gliomas. The model based on BTSC considers that only a specific, minority of tumor cells, which arise from mutations in stem or progenitor cells, have the ability to produce a tumor (Jordan, Guzman, & Noble, 2006; Pardal, Clarke, & Morrison, 2003; Reya, Morrison, Clarke, & Weissman, 2001). Biological similarities between the BTSCs and

neural stem cells were the first evidence shown by several studies for BTSC as a model of gliomas (Hemmati et al., 2003; Ignatova et al., 2002; Singh et al., 2003). There are three distinct properties of cancer stem cells including those of BTSCs: self-renewal, ability to differentiate into multiple lineages and extensive proliferative potential (Jhanwar-Uniyal, Labagnara, Friedman, Kwasnicki, & Murali, 2015). Similar to normal neural stem cells, BTSCs form free-floating neurospheres which can form new neurospheres supporting their stem-like nature.

The identification of the specific antigenic markers in GBM and the use of culture conditions initially used for neural stems cells were the first evidence for the presence of BTSCs (Piccirillo et al., 2009; Singh et al., 2004; Zeppernick et al., 2008). As it is illustrated in **Figure 3**, it has been shown that the regeneration of the tumor from BTSCs is largely associated with recurrence of GBM. Therefore, an important aspect of clinical treatment of GBM is targeting BTSCs.

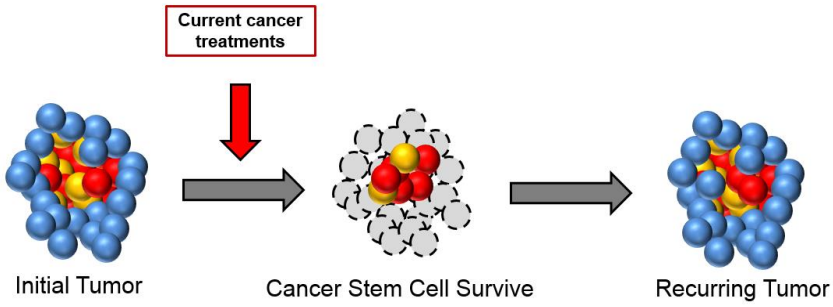

Figure 3. Brain tumor stem cells responsible for recurrence in GBM.

There are several targeting mechanisms that have been proposed for cancer stem cells. One of these proposed mechanisms is to make cells more amenable to other therapeutic agents by inducing differentiation. This approach was examined in a recent study which demonstrated that mTOR inhibition alone and in combination with differentiating agents can target cancer stem cells (M. D. Friedman, Jeevan, Tobias, Murali, & Jhanwar-Uniyal, 2013) leading to a decrease in cell proliferation. However, the real molecular target and the precise mechanisms of BTSC elimination in GBM are still unknown. Several of the proposed biomarkers (**Table 2**) were analyzed in BTSC in this thesis (data not shown).

Attribute	Marker
Cell surface protein	CD133, CD15, CD44, CXCR4, integrin alpha 6 (Jhanwar-Uniyal et al., 2015)
Cytoplasmic and nuclear protein	Nestin, Musashi-1, bmi-1 (Reya et al., 2001)
Transcription factor	SOX2, POU3F2, SALL2, OLIG2 (Suva et al., 2014)

Table 2. Properties of glioblastoma stem cells

1.5. Current therapeutic intervention and their limitations

The management of GBM begins with maximal surgical resection if feasible. The infiltrative nature of the tumor makes the complete resection almost always impossible. However, the surgical debulking not only provides tissue for histologic diagnosis and molecular studies but also does it lower the symptoms from mass effect. The extent of resection with current advances such as intraoperative mapping (Asthagiri, Pouratian, Sherman, Ahmed, & Shaffrey, 2007), fluorescence-guided surgery (Stummer et al., 2006), MRI-guided neuro-navigation and functional MRI have significantly improved providing increasingly safe surgical procedures. Nevertheless the surgical resections are not curative and in terms of the survival prolongation are, only modestly advantageous (Asthagiri et al., 2007; Lacroix et al., 2001; Stummer et al., 2006).

Radiotherapy (RT) is a post-surgical mainstay adjuvant treatment for malignant gliomas. The survival range is enhanced from 3 to 4 months to 7 to 12 months by addition of radiotherapy to the surgery (Stupp et al., 2005; Walker et al., 1978). The therapeutic effect of RT is limited, since by exceeding a certain dose, it can have cytotoxic effect on the normal cells leading to dramatic side effects. Additionally, 90% of the tumors recur at the original site after the standard RT (Hochberg & Pruitt, 1980).

In conjunction with the surgery and RT, chemotherapy with TMZ (an oral alkylating agent with good penetration through the BBB) increases the median survival to 14.6

months from 12.1 months (Stupp et al., 2005). However, the effectiveness of TMZ, the first line therapeutic drug, varies from patient to patient. Methyl guanine methyl transferase (MGMT) which is an important repair enzyme contributes to the resistance to TMZ (12.7 month survival). The epigenetic silencing of MGMT gene has increased the susceptibility of the tumor cells to TMZ (21.7 months survival) (Hegi et al., 2005). Despite these treatments, recurrence invariably occurs in malignant gliomas and TMZ has a limited activity in such patients (Yung et al., 2000). **Table 3** summarizes the available treatments and the most commonly used drugs.

Type of Treatment	**Example**
Convection-enhanced surgical delivery of pharmacologic agent	Cintredekin besudotox
Drugs to overcome resistance to TMZ	
MGMT inhibitors	O6-benzylguanine
PARP inhibitors	BSI-201, ABT-888
New chemotherapies	RTA744, ANG1005
Antiangiogenic therapies	
Anti-αvβ5	Integrins Cilengitide
Anti-hepatocyte growth factor	AMG-102
Anti-VEGF	Bevacizumab, aflibercept (VEGF-Trap)
Anti-VEGFR	Cediranib, pazopanib sorafenib, sunitinib, vandetinib, vatalanib, XL184, CT-322
Other agents	Thalidomide
Targeted molecular therapies Akt	Perifosine
EGFR inhibitors	Erlotinib, gefitinib, lapatinib, BIBW2992, nimotuzumab, cetuximab
FTI inhibitors	Tipifarnib, lonafarnib

HDAC inhibitors	Vorinostat, depsipeptide, LBH589
HSP90 inhibitors	ATI3387
Met inhibitors	XL184
mTOR inhibitors	Everolimus, sirolimus, temsirolimus, deforolimus
PI3K inhibitors	BEZ235, XL765
PKCβ	PKCβ Enzastaurin
PDGFR inhibitors	Dasatinib, imatinib, tandutinib
Proteasome	Bortezomib
Raf inhibitors	Sorafenib
Src	Dasatinib
TGF-β	AP12009
Combination therapies	Erlotinib plus temsirolimus, gefitinib plus everolimus, gefitinib plus sirolimus, sorafenib plus temsirolimus, erlotinib, or tipifarnib, pazopanib plus lapatinib
Immunotherapies Dendritic cell and EGFRvIII peptide vaccines	DCVax, CDX-110
Monoclonal antibodies	^{131}I-anti-tenascin antibody
Other Therapy	^{131}I-TM-601

Table 3. Selected treatments for Malignant Gliomas.

EGFR denotes epidermal growth factor receptor, FTI farnesyltransferase, HDAC histone deacetylase, HSP90 heat-shock protein 90, MGMT O6-methylguanine−DNA methyltransferase, mTOR mammalian target of rapamycin, PARP poly (ADP-ribose) polymerase, PDGFR platelet-derived growth factor receptor, PI3K phosphatidylinositol 3-kinase, PKCβ protein kinase C β, TGF transforming growth factor, TMZ, and VEGFR vascular endothelial growth factor receptor. Reproduced with permission from (Wen & Kesari, 2008), Copyright Massachusetts Medical Society. (Chi & Wen, 2007; Furnari et

al., 2007; Sathornsumetee, Reardon, et al., 2007; Sathornsumetee, Rich, & Reardon, 2007).

1.6. Carbonic anhydrase IX as a drug target

A common feature of the solid tumors is their hypoxic environment which is as a result of structurally abnormal and functionally unstable tumor vasculature leading to a poor oxygen delivery to the growing tumors of high oxygen demand (Bailey, Wojtkowiak, Hashim, & Gillies, 2012; Lendahl, Lee, Yang, & Poellinger, 2009). To grow and to survive in this hostile environment, a highly conserved hypoxia-induced intracellular signalling cascade regulated by transcription factor hypoxia inducible factor 1 and 2 (HIF1/2) is activated by the stressful hypoxic cells in the tumors (Lendahl et al., 2009). HIF pathway activation leads to modulation of many genes involved in critical processes which regulate tumor progression (Brahimi-Horn, Bellot, & Pouyssegur, 2011; Gillies, Robey, & Gatenby, 2008). CA IX shows the most dramatic transcriptional activation among the genes that are targeted for upregulation by HIF pathway in cancer cells (Kaluz, Kaluzova, Liao, Lerman, & Stanbridge, 2009; McDonald, Winum, Supuran, & Dedhar, 2012).

CA IX is highly expressed in a systemic and robust manner in cancer cells pointing its importance for adaptation of the cells in the aberrant oxygen status within tumors. CA IX is an integral transmembrane enzyme which is composed of 4 domains: the N-terminal proteoglycan domain controlling cell attachment (Zavada et al., 2000), the extracellular catalytic domain, a hydrophobic transmembrane region, and a cytoplasmic tail (Opavsky et al., 1996).

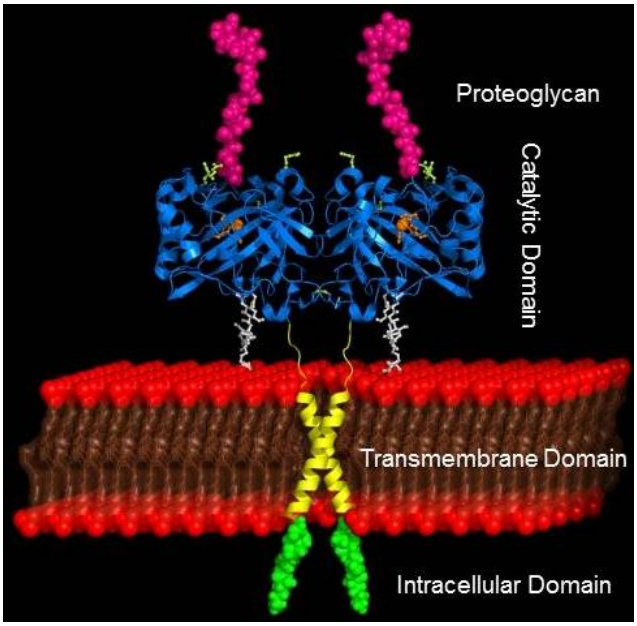

Figure 4. The structural arrangement of the full length CA IX dimer on the cellular membrane.

Adapted from (Alterio et al., 2009). Copyright (2009) National Academy of Sciences, USA.

CA IX catalyzes the reversible conversion of carbon dioxide to carbonic acid (CO_2 + H_2O to HCO_2^- and H^+). Among all human α-CAs, CA IX has the highest catalytic activity and the exposure of its catalytic domain to the extracellular domain allows its contribution to the intra-extracellular pH (Swietach, Vaughan-Jones, & Harris, 2007; Wingo, Tu, Laipis, & Silverman, 2001). CA IX plays critical roles in the tumor cells including cell survival and proliferation, stem cell phenotype maintenance (Lock et al., 2013), epithelial-mesenchymal transition (EMT) in carcinoma cells (Fiaschi et al., 2013), invasion, metastasis, and resistance to radiation therapy and chemotherapy (Dubois et al., 2011; Ivanov et al., 2001; Potter & Harris, 2004; Proescholdt et al., 2012; Robertson, Potter, & Harris, 2004). More importantly, the accumulation of the by-products such as lactic acid produced by highly metabolic cancer cells involved in glycolytic metabolism leads to the presence of an increasingly acidified intracellular pH and basic extracellular pH (Gillies et al., 2008; Parks, Chiche, & Pouyssegur, 2011). CA IX, highly upregulated under such conditions, acts as an essential component of a complex cellular system

involving several proteins and buffer systems responsible for the intra-extracellular pH homeostasis.

Several studies have established that depletion of CA IX gene expression and inhibition of its catalytic activity in the context of hypoxia dysregulates pH homeostasis and affects the viability of several types of cancer cells *in vitro* (Proescholdt et al., 2012; Robertson et al., 2004). Multiple studies in several human tumor cell lines with constitutive CA IX expression or upregulated CA IX expression under hypoxia, have demonstrated that selective CA IX inhibitors induce decline in intracellular pH (acidification) and enhancement of the extracellular pH (alkalinisation) (Cianchi et al., 2010; Dubois et al., 2007; Dubois et al., 2011; Y. Li et al., 2009; Lou et al., 2011).

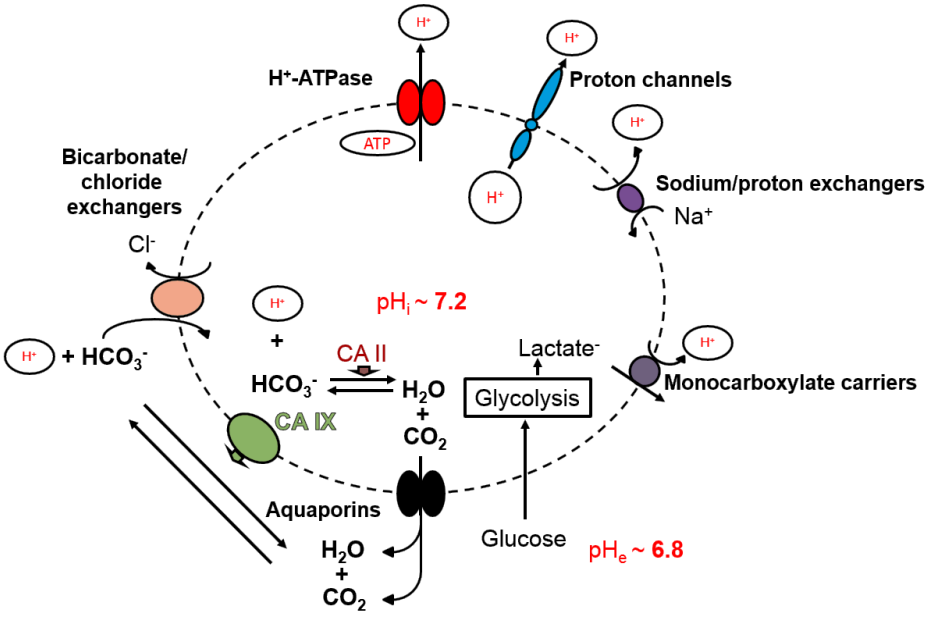

Figure 5. Molecular mechanisms of proton extrusion/secretion from cancer cells mediated by CAs.

Adapted from (Ivanov et al., 2001) with permission from Elsevier.

Tumor growth is tightly related to the cell to cell interactions as well as their microenvironment which is acidic with varying hydrostatic and oxygen pressures (Helmlinger, Yuan, Dellian, & Jain, 1997; R. K. Jain, 1999). As illustrated in **Figure 5**, the pH homeostasis is tightly controlled by proton extrusion mechanisms which mostly

require energy consumption for proper functioning. More importantly, the cell surface CA IX plays a critical role in regulation of proton and bicarbonate in the close vicinity of the tumor cells maintaining an acidic pH_e and an alkaline pH_i. It has been proposed that CA IX is a pH sensing enzyme due to the presence of histidine residues in the catalytic domain outside as well the cytoplasmic domain inside the cells (Wingo et al., 2001). In differentiated GBM, CA IX is almost exclusively localized in the cells specialized in acid/base homeostasis (gastrointestinal track), lends support to this hypothesis about CA IX (Ivanov et al., 2001).

1.7. Rationale for selecting CA IX as a therapeutic target in GBM

CA IX is an especially attractive target in GBM because of several reasons: firstly, CA IX is expressed in GBM and the degree of its expression exhibits close correlations with the degree of invasiveness. It is an independent negative factor for poor overall survival (OS) in patients with GBM (Proescholdt et al., 2012). Secondly, it provides functions critical for tumor growth and metastasis, including pH regulation, survival and adhesion/migration. Thirdly, it has an amino acid sequence at the extracellular surface of cell membrane readily accessible to antibodies or small molecule inhibitors. Finally, it is selectively expressed by GBM tumor cells and shows highly restricted expression in normal brain tissue, offering the possibility of selective targeting of the cancer (Proescholdt et al., 2005).

CA IX inhibition leads to a significant decrease in the catalysis of carbon dioxide and water reaction to proton and bicarbonate. Inhibition of such reaction and the consequent decrease in proton production contribute to a decrease in extracellular acidity. On the other hand, the decrease in bicarbonate production and its transport to the intracellular milieu leads to an increase in intracellular acidity. Bicarbonate is normally transported to the cell and reacts with a proton, a reaction catalyzed by CA II, and produces water and carbon dioxide which are transported to the extracellular milieu via aquaporins. In this way, protons are extruded from the intracellular environment to the stroma maintaining the pH homeostasis in the tumor cells ($H_2O + CO_2 \rightarrow HCO_3^- + H^+$).

TMZ is the first line therapeutic against GBM. It is a prodrug whose activation is highly pH dependent. In the alkaline pH (7.2-7.4), it is spontaneously converted to MTIC (5-(3-

methyltriazen-1-yl) imidazole-4-carboximide), its active form which acts as an alkylating agent (H. S. Friedman, Kerby, & Calvert, 2000). However, TMZ has a very poor effectiveness and it is essential to find sensitizers which can enhance its therapeutic effect.

CA IX seems to act against the activation of TMZ by acidification of the extracellular milieu. Thus, based on the characteristics of TMZ and the functions of CA IX, we hypothesized that the inhibition of CA IX by ATZ (ATZ- a non-specific CA IX inhibitor) and a humanized monoclonal antibody raised against catalytic site CA IX will enhance the effectiveness of TMZ in the GBM monolayers (2D) and the spheroid (3D) cell models.

Chapter 2: Materials and Methods

Solutions, media and reagents

3-(4,5-Dimethylthiazol-2-yl)-2,5-diphenyl tetrazolium bromide (MTT), Hoechst 33342, Propidium Iodide (PI), ATZ (A6011-10G), Temozolomide (T2577), goat serum (G-9023) were purchased from Sigma- Aldrich (Oakville, ON, Canada). U251N acquired in October 2010 from Dr. Josephine Nalbantoglu (MNI, Neuroimmunology Unit, Webster Pavillion; rmW010K). U251N cell line was originally obtained from the American Type Culture Collection. Human IgG1 Anti-CA IX (1.8 mg/mL, Ab ~ 150 KD) was acquired from Dr. Nathan Yoganathan (Kalgene Pharmaceuticals, Kingstone, Ontario). Mouse anti-human CA IX-Mab was acquired from ABCAM (ab107257). Cell culture media, penicillin–streptomycin, and heat-inactivated fetal bovine serum (FBS) were purchased from Invitrogen (Burlington, ON, Canada).

Cell culture

U251N human GBM monolayers were cultured in Dulbecco's Modified Eagle Medium (DMEM; Gibco, Life Technologies Inc., Burlington, ON, Canada) supplemented with 1% (v/v) FBS (Gibco) and 1% (v/v) penicillin–streptomycin (Gibco). Cells were seeded 24 h before treatment according to the appropriate density for the indicated assay (described in detail below). They were maintained at 37 °C with 5% CO2 and 95% relative humidity.

BTSC culture

Human GBM stem cells (hGSC) were isolated as previously performed (Kelly et al., 2009) and expanded in neurosphere cultures. HGSC spheres are cultured in complete Neurocult-NS-A proliferation medium (Neurocult basal medium containing: Neurocult NS-A proliferation supplement, 20 ng/ml rh EGF, 20 ng/ml rh bFGF and 2 µg/ml Heparin) from Stem Cells Technologies. When spheres appear large enough for passaging (<300 µm in diameter), they were collected in tubes and spun at 200 g for 3 minutes. To dissociate the spheres, 800ul of Accumax (Millipore) was added to the cell

pellet and incubated for 5 minutes at 37°C, they were then washed with PBS, centrifuged and re-suspended in complete Neurocult-NS-A proliferation medium and seeded at a concentration of 200 000 cells/flask.

Spheroid formation

Spheroid cultures were prepared using a protocol adapted from the liquid overlay system previously established by Dhanikula et al. (Dhanikula, Argaw, Bouchard, & Hildgen, 2008): confluent U251 monolayer cell cultures were detached using 0.05% trypsin-EDTA (Gibco), and seeded at 5,000-50000 cells per well in 96-well plates pre-coated with 2% agarose (Invitrogen) in serum-deprived DMEM solution. Spheroids were seeded and maintained in filtered (0.22 µm) complete DMEM medium for four days before drug treatment with ATZ (alone or encapsulated in micelles), TMZ and the Mab-CA IX. For spheroids older than 4 days, 100 ul of filtered and complete DMEM medium was added to each well followed by 100 ul removal of the medium from each well every four days.

ATZ incorporation into polymeric nano-particles

ATZ-loaded micelles were prepared by dissolving Poly-(ethylene glycol) methyl ether-block-poly-(lactide-co-glycolide) (PEG-PLGA) and ATZ in tetrahydrofuran (THF) with some sonication (3 mins) to obtain a clear solution (10 mg/ml of ATZ and PEG-PLGA). An equal volume of water was placed in a vial with a magnetic stirrer. The THF solution containing polymer alone or a mix of polymer-drug was added drop wise into the water under constant agitation (10 µl/s). The vial was left open with constant agitation for 24 hours. The remaining THF was removed in vacuum. The excess non-encapsulated ATZ was removed by centrifugation (10 min, 1000 g), and its mass was determined after freeze-drying to remove any trace of water.

The size of the blank and ATZ-loaded micelles was determined by asymmetrical flow field-flow fractionation (AF4, Dualtec, Wyatt Corporation, Santa Barbara, CA, USA) coupled to a UV-Vis detector set at 250 nm and a dynamic light scattering detector (DLS).

Cell treatment

Confluent monolayer cell cultures were detached using 0.05% trypsin-EDTA, and seeded in 24-well-plate (Costar) at 20,000, 10,000 or 5000 cells per well (for 1, 3 and 6 days treatments respectively) or seeded in 6-well plates (Corning) at 300,000 or 100,000 cell per well (for 1 and 6 days treatments respectively), and treated after 24 hours.

For chemical induction of hypoxia, cells were treated with 50 μM $CoCl_2$ (DBH- 27790) dissolved in sterile pure water, for 24 hours before addition of temozolomide (100 μM), ATZ (100 μM), Mab-CA IX (5 nM) or their combinations (for 1-6 days treatments). Spheroids were treated the same as monolayers excluding the addition of $CoCl_2$. Stock solutions of temozolomide (Sigma-Aldrich; 43 mM), ATZ (Sigma-Aldrich; 200 mM) were prepared in dimethyl sulfoxide (DMSO; Sigma-Aldrich), and were added to cells for a final DMSO concentration of <0.5%. $CoCl_2$ was dissolved in pure water. Mab-CA IX (Kalgene; 12 μM) stock was dissolved in PBS.

MTT assay

Following treatment, the culture medium was replaced with serum-deprived DMEM containing thiazolyl blue tetrazolium (MTT, 0.5 mg/ml; Sigma Aldrich). The cells were incubated at 37 °C for 60 minutes to allow for formazan formation, after which the medium was removed, and dimethyl sulfoxide (DMSO; 500 μl; Sigma Aldrich) was added to dissolve the formazan crystals. Samples were collected in triplicate, and the absorbance was measured at 595 nm using a microplate reader (Benchmark; Bio-Rad).

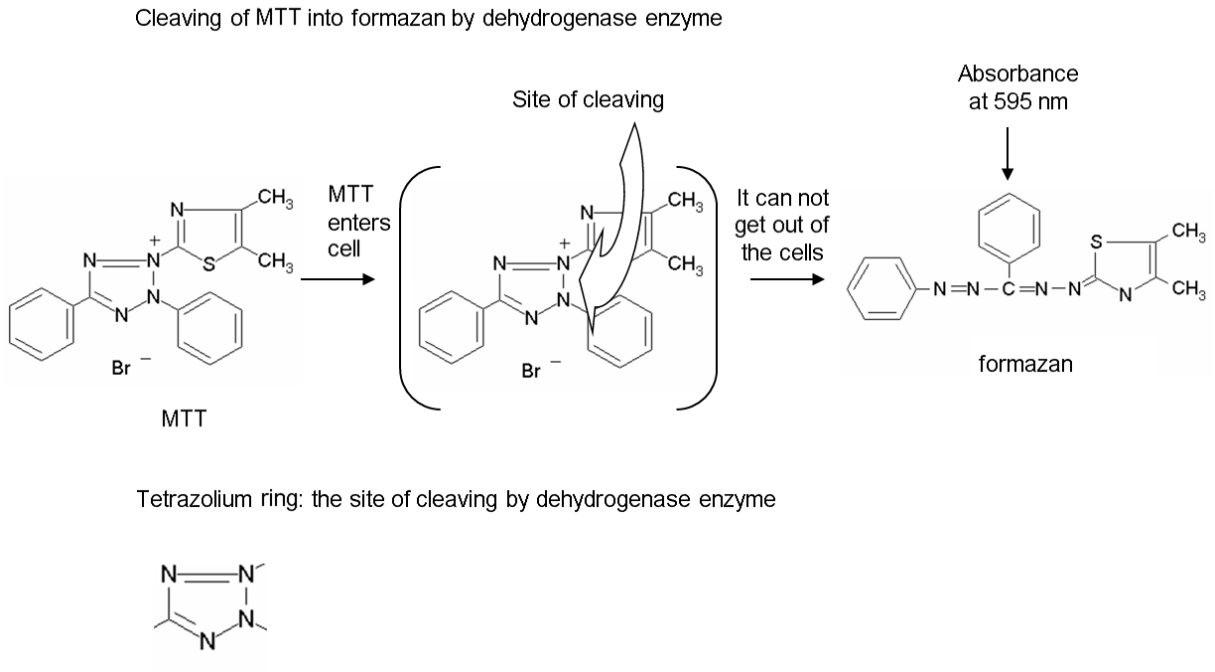

Figure 6. Colorimetric assay for measurement of mitochondrial metabolic activity.

XTT assay

BTSCs were plated at 10 000 cells/well in 96 well overnight in culture media. Drugs (ATZ, TMZ and ATZ-micelles) were added to their final concentrations in a final volume of 200 µl. After indicated time of incubation at 37°C, 50 µl of XTT was prepared as manufacture's instruction (Life Technologies) and the mix XTT solution was added and further incubated for 2 hours at 37°C. The absorbance at 490 nM was measured on an Epoch plate reader.

Hoechst 33342 and Propidium Iodide labeling

In monolayer cultures, Hoechst 33342 (10 µM) and PI (1.5 µM) were added to the culture medium following the treatments and incubated at 37 °C for 60 minutes. Analysis of the plates was immediately followed. Cell imaging was conducted using an automated microscopy platform (Operetta High Content Imaging System; Perkin Elmer). Image analysis and cell counting was performed using the Columbus Image Data Storage and Analysis platform (Perkin Elmer).

In spheroid cultures, Hoechst 33342 (10 μM) and PI (1.5 μM) fluorescent dyes were added 4h prior to measurements. Following treatment, individual spheroids were carefully transferred onto a microscope slide using a pipette, and flattened under a coverslip. Imaging was conducted using fluorescence microscope (Leica), and fluorescence intensity was quantified using ImageJ software.

Caspase-3 activity measurement

EnzCheck caspase-3 assay kit #2 (E13184) with some minor changes to its protocol was used to measure caspase-3 activity as described below. Following the treatments, the culture medium was collected. Cells were then washed with PBS (2X) and detached using 0.05% trypsin-EDTA. The cells were then collected and added to their respective culture medium. Then they were centrifuged at 11000 g for 4 mins. Then 50 µl of the 1X lysis buffer (1.5 mL of 200 mM TRIS, pH 7.5, 2 M NaCl, 20 mM EDTA, 0.2% TRITON™ X-100) was added to each pellet and re-suspended. The suspension of cells was then frozen at -80 and thawed subsequently. Then they were centrifuged at 11000 g for 4 mins. 50 µl of the supernatant from each treatment was then transferred to a 96 well plate (Sarstedt). then 50 µl of the reaction buffer (50 mM PIPES, pH 7.4, 10 mM EDTA, 0.5% CHAPS) at 5X diluted down to 2X by dH_2O containing 20mM DTT was added to each supernatant followed by 30 mins incubation at RT. The controls contain 50 µl of the lysis buffer and 50 ul of the reaction buffer (2X) with 10 mM DTT. The fluorescence is then measured (excitation/emission ~496/520 nm) using the appropriate excitation and emission filters by a spectrofluorometer (FLUOstar OPTIMA).

Western blotting

U251N GBM cells were seeded at a density of 300 000 per well into six-well cell culture plates and left to adhere for 24 h in a final volume of 2 ml serum-supplemented DMEM media (10% FBS, 1% Pen-Strep). The drugs and the nano-carriers were added to the adherent monolayers in the concentrations ranging from 10-100 μM for 1-6 days as indicated in individual figure legends. Following treatment, cells were trypsinized, pelleted, resuspended in lysis buffer (10mM Na Phosphate pH 7.0, 150 mM NaCl, 1% NP40, 0.1% SDS, 1% Na Deoxycholate, 10 mM NaF, 2 mM EDTA), centrifuged and

followed by the collection of the supernatant. For spheroids, following the treatments, they were picked up by a pipette and pelleted and resuspended in the lysis buffer. Of the total cell extracts, 10-20 mg of protein (measured by protein assay (BIO-RAD)) was loaded onto a 12% gradient sodium dodecyl sulfate-polyacrylamide gel electrophoresis and transferred to a PVDF membrane. Membranes were washed with 0.1% Tween-20þTBS and blocked with 3% milk (with 1:10000 of 10% NaN_3)+0.5% Tween-20+TBS for 1h at room temperature (RT) and incubated with primary antibodies diluted 1:1000–5000 in blocking solution overnight at 4 °C. After three washes with 0.1% Tween-20+TBS, the membranes were incubated with the HRP-conjugated anti- rabbit/mouse (Bio-Rad) diluted 1:5000 in 3% milk (with 1:10000 of 10% NaN_3)+0.5%Tween-20+TBS for 1 hour at RT. After three washes with 0.1% Tween-20+TBS,HRP substrate (Luminata, Millipore, Billerica, MA, USA) was added and incubated for 5 min, following which the membranes were exposed to film (Harvard, Holliston, MA, USA). Blotting with mouse anti-actin (dilution 1:5000, Millipore, Burlington, MA, USA) was used as a housekeeping protein to control for global protein expression levels. Densitometry was performed using ImageJ (NIH, Bethesda, MD, USA), and data were tabulated and graphed using the Microsoft Excel.

Statistical analysis

Data was graphed and tabulated using Microsoft Excel®. Each experiment was performed at least two times. Each treatment was performed in triplicates (24-well plates), or in five or six samples (96-well plates). All data are expressed as mean ± S.E.M. The student's t-test with Bonferroni correction was used to analyze significant differences between two group means (p values < 0.05 were considered to be significant) using GraphPad Prism®.

Chapter 3: Results

3.1. CA IX inhibition in GMB monlayers

CA IX was proposed as a biomarker of hypoxia in several tumor types (Bernstein, Andrews, Slevin, West, & Homer, 2015). In order to establish the hypoxic conditions in monolayer GBM cells U251N, $CoCl_2$ (10-100 μM) was used in different concentration as an inducer of chemical hypoxia (**Figure 7A**). CA IX expression was assessed by western blotting using antibodies recognizing CA IX and the expression is presented relative to the control cells not exposed to CoCl2 (**Figure 7**). Although the degree to which CA IX is expressed in U251N monolayers was undetectable under normoxic conditions with and without ATZ (100 μM) treatment, CA IX expression was significantly ehnaced at concentrations as low as 10 μM ($p<0.01$) after 3 days of treatment (**Figure 7B**) under hypoxic conditions. $CoCl_2$, enhanced CA IX in a dose dependent manner (**Figure 7B**). CAIX expression induced by $CoCl_2$ was supressed when cells were treated concomitantly with ATZ (**Figure 7B**).

A

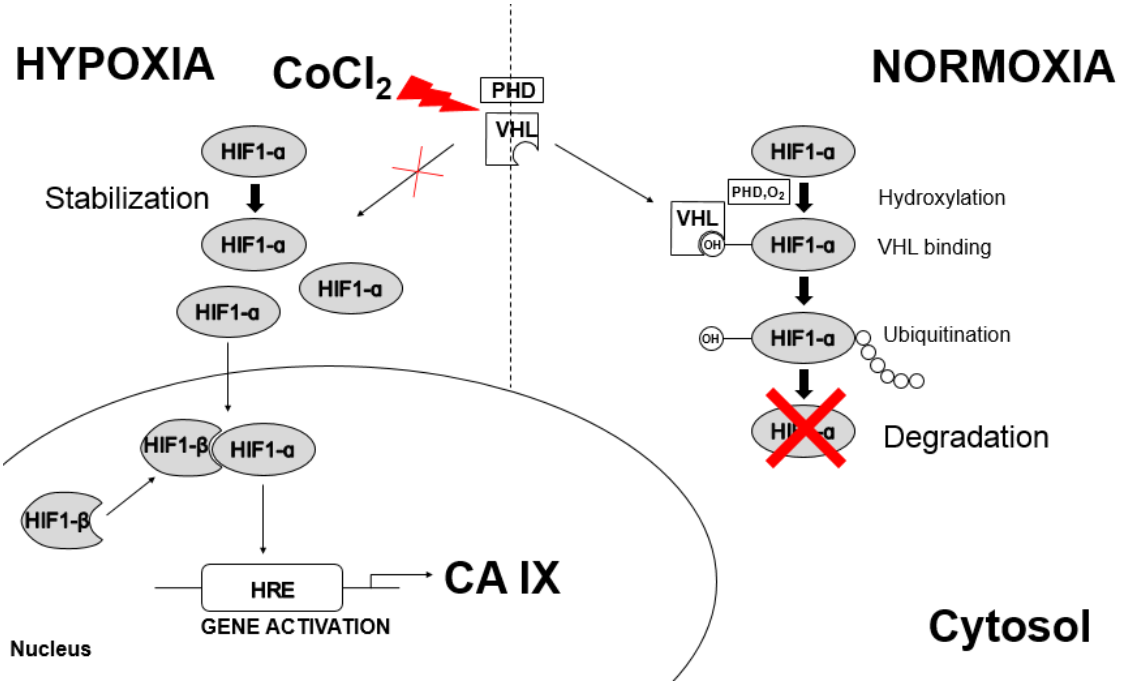

B

CoCl2 µM	50	50	0	0	10	50	100
ATZ µM	1	100	0	100	0	0	0

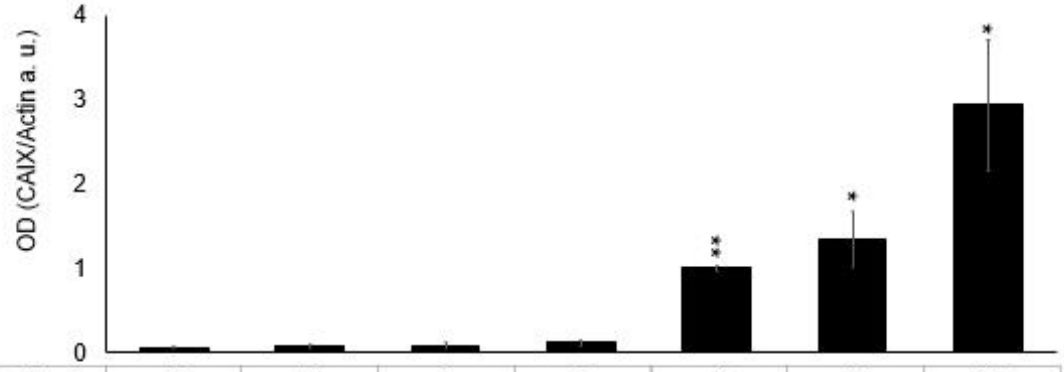

$CoCl_2$ µM	50	50	0	0	10	50	100
ATZ µM	1	100	0	100	0	0	0

Figure 7. Induction of hypoxia and expression of CA IX in U251N glioblastoma monolayers.

(A) Induction of CA IX upon exposure to $CoCl_2$ is illustrated. Based on studies by (Pastorekova, Ratcliffe, & Pastorek, 2008) with permission from Elsevier. (B) Induction of CA IX in U251 GBM monolayers. U251N monolayers were grown on a 6 well plate for 24 hours in serum containing DMEM. They were then treated with $CoCl_2$ (10-100 μM) and ATZ (1 & 100 μM) alone or with their combinations (concomitantly) for the total of 3 days. Following the treatments, the total cell lysate was collected and immunoblotted for CA IX expression. The Level of expression of CA IX is presented as the optical density of the bands over their respective actin band, the loading control (10 μg), on the ordinate. The abscissa shows the concentrations of the drug treatments as indicated. The results are representative of three independent experiments. Statistically significant differences from control were calculated using a t-test and are indicated by * ($p<0.05$), ** ($p<0.01$).

Having established the appropriate hypoxic conditions for CA IX induction in monolayers, we then investigated the relationship between the CA IX expression in and cell viability in U251N cultures in the presence and absence of CAIX inhibitor ATZ.

U251N cell viability (in the monolayers) did not significantly change upon exposure to the drug treatments under normoxia or hypoxia within the initial 24 hours following ATZ (100 μM), TMZ (100 μM) and their combination treatment. (**Figure 8B**). However, after three days of exposure to TMZ alone or in combination with ATZ (100 μM) or the anti-CA IX antibody (5nM) , there was a reduced cell viability only under hypoxia to 47 ± 5 ($p<0.05$), 44 ± 6 ($p<0.05$), and 39.8 ± 0.4 ($p<0.01$) respectively (**Figure 8B**). Although ATZ treatment for 6 days did not significantly decrease cell viability under normoxic and hypoxic conditions, it caused a significant cell death when combined with TMZ (100 μM), under both conditions (**Figure 8B**). The reduction in cell viability is moderately, but significantly higher, for ATZ (100 μM) and TMZ (100 μM) combined when compared to the TMZ (under normoxic (19 ± 2 ($p<0.05$) and 25 ± 2 ($p<0.05$) respectively) and hypoxic conditions (13.9 ± 0.6 ($p<0.01$) and 20 ± 2 ($p<0.01$) respectively). Photomicrographs (**Figure 8A**) indicate some picnotic and hypertrophic nuclei labeled with PI, suggesting several modes of cells death caused by the treatments. Measurements of mitochondrial

metabolic activity in U251N cells treated with the aforementioned drugs revealed a similar pattern of reduction to that of cell counting indicating a strong dependence of cell viability on mitochondrial functions (**Figure 8C**).

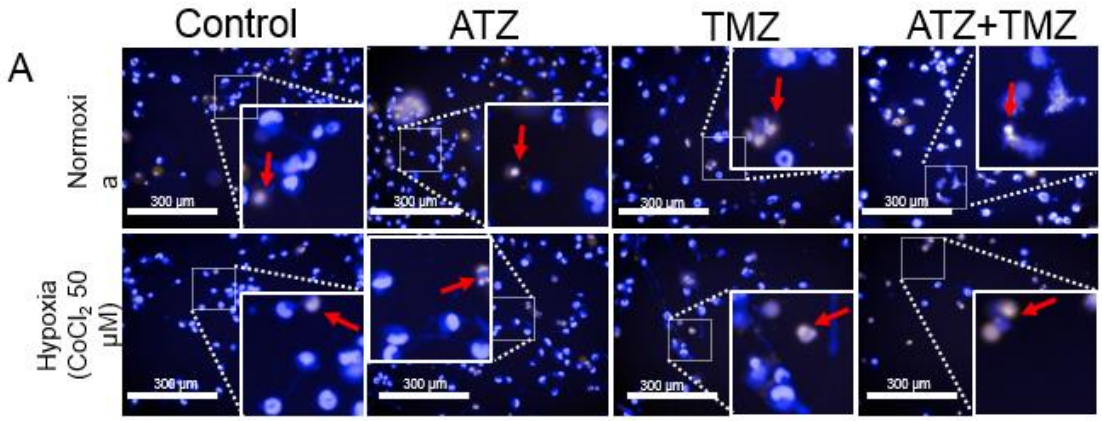

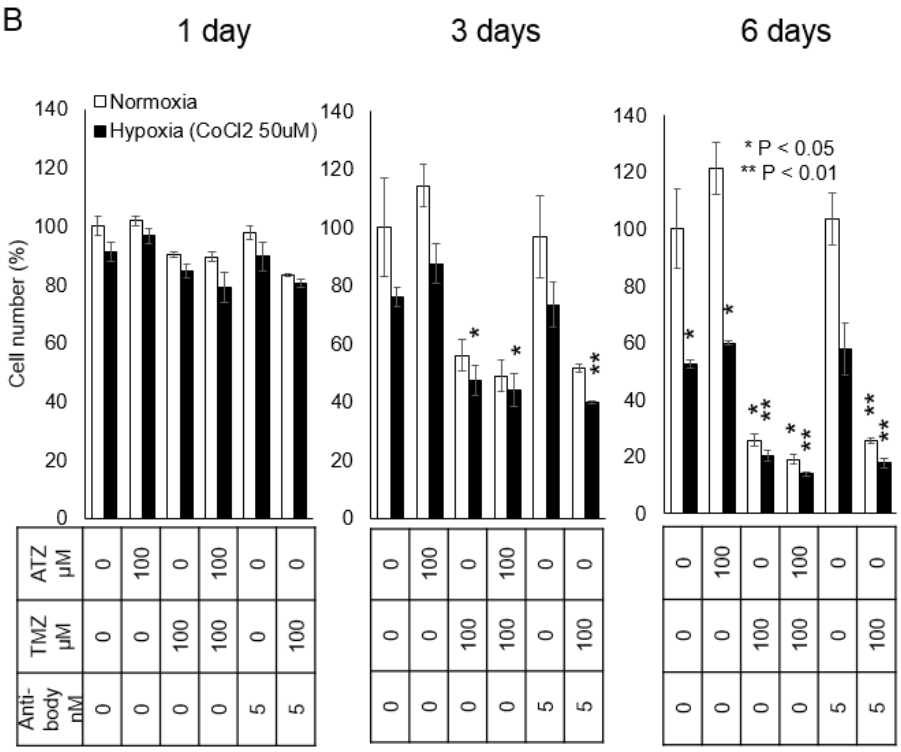

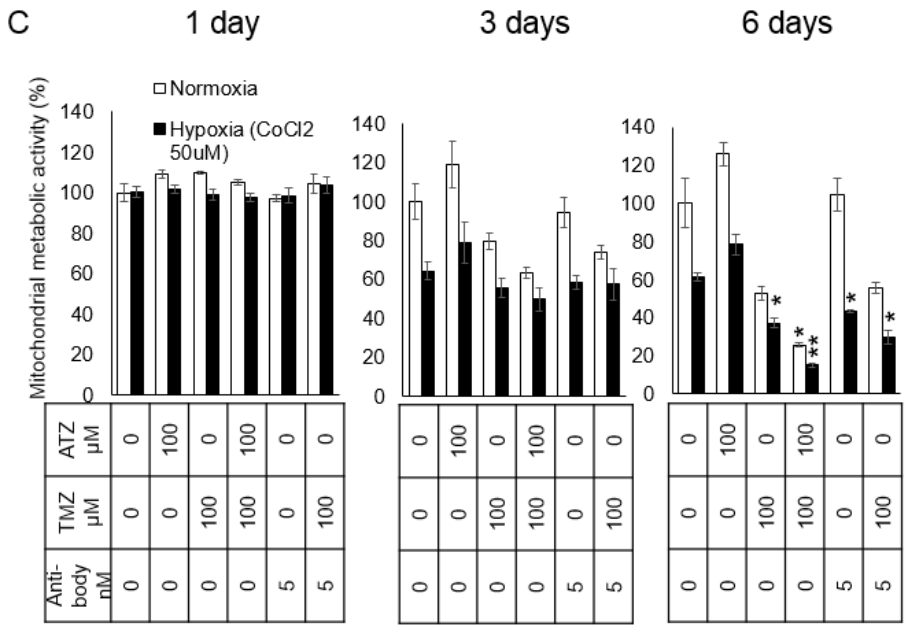

Figure 8. CA IX inhibition combined with TMZ treatment moderately compromises viability in U251 monolayers.

(A) Photomicrograph of U251N treated cells labelled with Hoechst-33342 and PI. U251N monolayer were grown (20000, 10000 and 5000 cells for 1, 3 and 6 days treatments respectively) in 24-well-plates in serum containing DMEM for 24 hours. Cells were either exposed or not (control) to CoCl2 (50 µM) for 24 hours to induce hypoxia. ATZ (100 uM), anti-CA IX antibody (5 nM), TMZ (100 uM) and their combinations (concomitantly) were then added and kept for 1, 3 and 6 days. Following the treatments, Hoechst 33342 and PI were added and then cell imaging was conducted, by an automated microscopy platform. The red arrows show the PI positive cells. (B) Quantitative data for cell viability are expressed as cell number (%) relative to the untreated cells (controls). Image analysis and cell counting was performed using the Columbus Image Data Storage and Analysis platform (Perkin Elmer). Average values and S.E.Ms. are reported for triplicate measurements. Results are representative of at least two independent experiments. (C) Mitochondrial metabolic activity (%) of U251 cells exposed to drugs for 1-6 days. Upon the end of the treatments, the culture medium was replaced with serum-deprived DMEM containing thiazolyl blue tetrazolium. Samples were collected in triplicate, and the absorbance was measured at 595 nm

using a microplate reader. Average values and S.E.Ms. are reported for triplicate measurements which were repeated at least twice. Statistically significant differences from control were calculated using a t-test and are indicated by * ($p<0.05$), ** ($p<0.01$).

3.2. Establishment of spheroids with intrinsic CA IX expression

Although the induction of hypoxia by $CoCl_2$ creates a condition and a model relevant for the hypoxic cells in the tumor cores it is still not representing the intrinsically hypoxic tumor cells in the core of the tumor. We therefore established conditions for spheroid formation with GBM cells in 3D. Representative spheroids formed from different cell number and at different times are shown in **Figure 9**. These spheroids contain hypoxic cores as the *in situ* GBM tumors. Spheroids seeded with smaller number of cells (5000 cells) grew at much faster than those formed from larger number of cells (10000 and 20000 cell) (**Figure 9A**). Regardless of the initial number of seeded cells, the growth rate dramatically dropped once the spheroids reached a certain volume (~8 x 10^6 μm^3) after 7 days (**Figure 9B**).

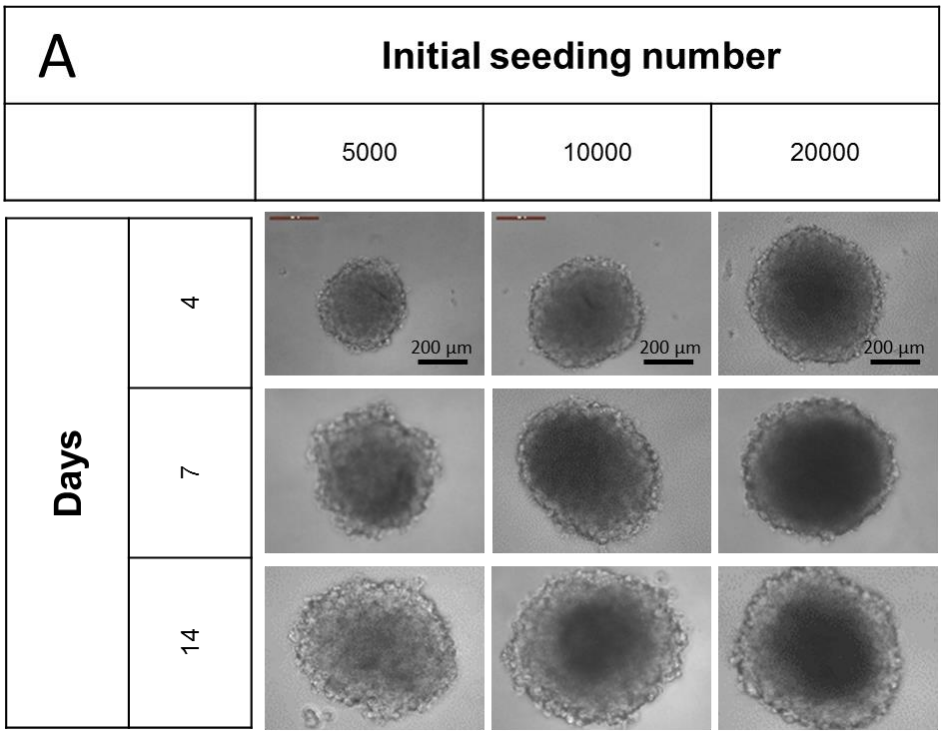

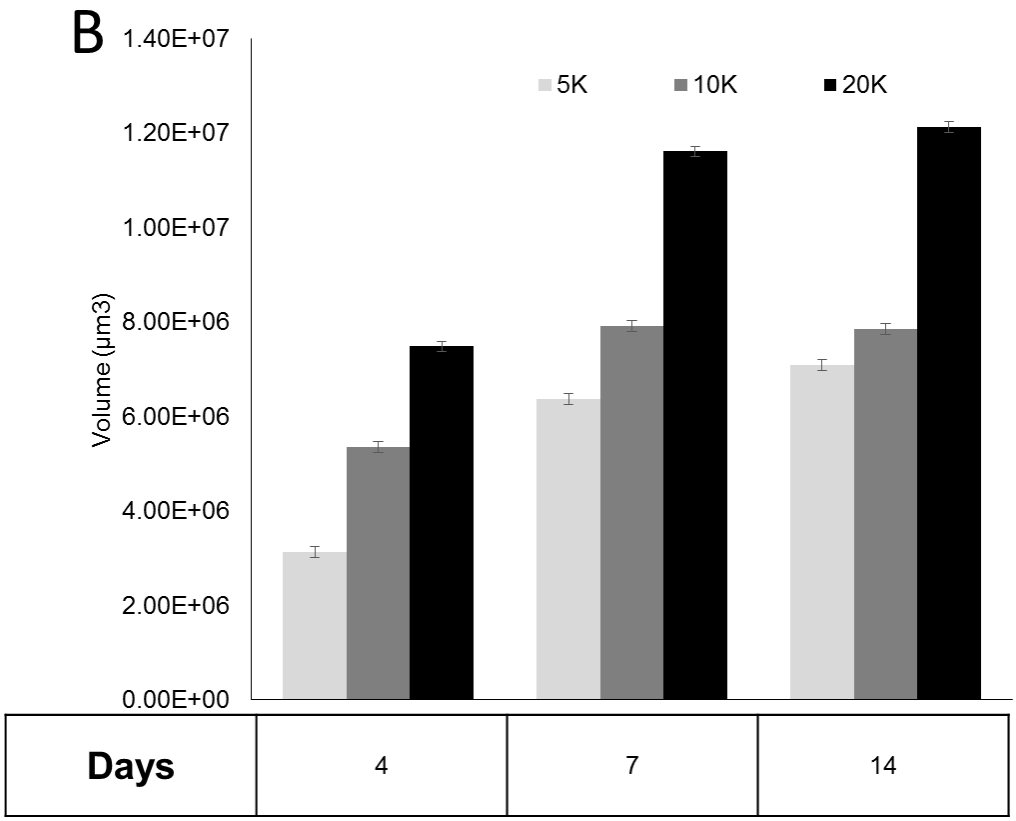

Figure 9. Spheroids establishment at different times and cell numbers.
(A) Morphology and the sizes of the spheroids. Spheroids were developed from indicated initial cell numbers (from 5000-20000) at different time periods (4 to 14 days) as described in material and method section. (B) Quantitative data for the spheroids volumes expressed as μm^3 in the ordinate. The volumes are estimated using the spheroids diameter and depth. Bright field microscopy was used to image the spheroids. Scale bars in the top row are representative for all panels shown. Average values are reported for N=10.

Having seen the increase in the size of spheroids over time (**Figure 9**), we assessed CA IX expression and related it to the spheroid sizes and duration of their growth. Cell lysates collected from U251N spheroids of different sizes (i.e. different cell number from 5000 to 20000) and grown over different time periods (4-16 days) were analyzed by Western blots. CA IX was expressed in all spheroids but the level of expression was clearly cell number and time dependent. (**Figure 10A and 10B**). The most significant

CA IX expression was found in spheroids made of 50000 cells and those which were grown over 16 days (**Figure 10B**) (p<0.01).

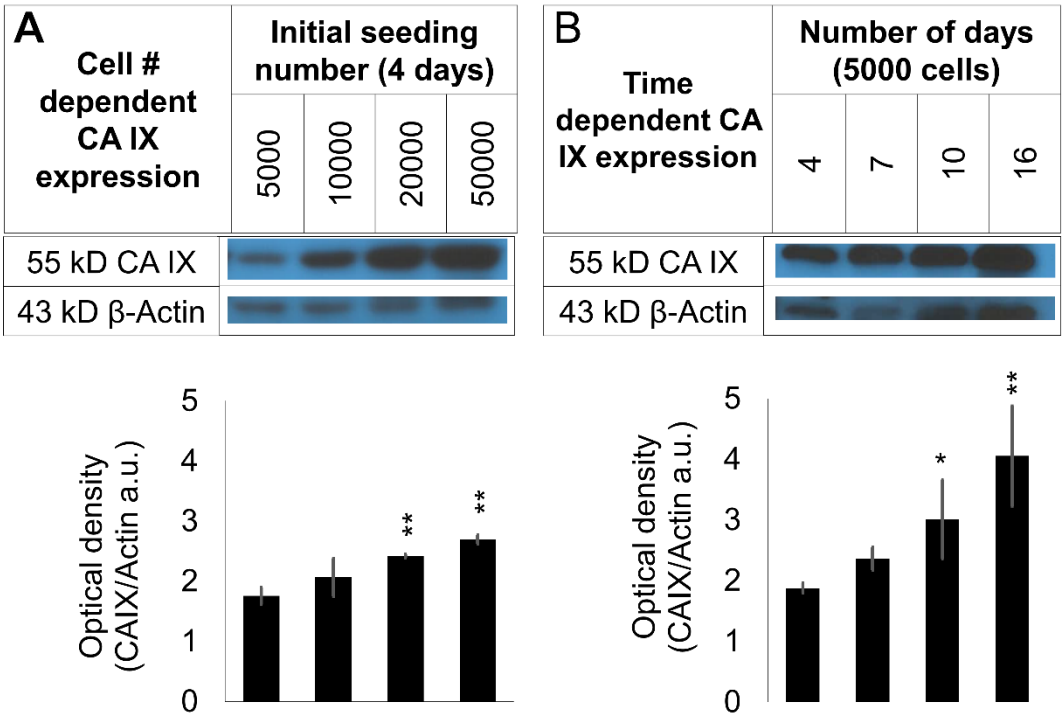

Figure 10. Time and size-dependent enhancement of CA IX expression in glioblastoma spheroids with hypoxic cores.

(A) Cell number dependent CA IX expression in U251N spheroids. U251 spheroids were developed in 96-well plates pre-coated with 2% agarose (in DMEM) in serum containing DMEM at the indicated cell numbers for 4-16 days. Spheroids were then picked up by a pipette and centrifuged. Total cell lysate was collected and immunoblotted for CA IX. (B) Time dependent CA IX expression in U251N spheroids. The Level of expression of CA IX is presented as the optical density of the bands over their respective actin band, the protein loading control (20 µg), on the ordinate. The abscissa shows the number of cells and days at which the spheroids were developed. The results are representative of at least two to three independent experiments. Statistically significant differences from control were calculated using a t-test and are indicated by * (p<0.05) and ** (p<0.01).

Next, upon establishment of CA IX expression in the spheroids we hypothesized that inhibition of CA IX in the U251N GBM spheroids (with high CA IX expression) will enhance the cell killing. Therefore, the spheroids were treated with inhibitors of CA IX, ATZ (100 μM) and anti- CA IX antibody (5 nM), alone or in combination with TMZ (100μM) for 1-6 days. One day treatments did not increase cell death relative to that of the control (**Figure 11B**). After 3 days of drug treatments differences in viability were obvious: ATZ or TMZ alone did not enhance cell death but when they were combined they caused a significant increase in cell death (0.38 ± 0.02 a.u., $p<0.05$). Similarly, ATZ (100μM) treatment did not augment cell death after 6 days treatment but when combined with TMZ, it significantly enhanced the cell death (1.28 ± 0.06 a.u., $p<0.0001$). Although TMZ alone after 6 days treatment did cause a significant cell death, ATZ significantly enhanced its killing effect ($p<0.001$). In contrast, the treatments with the antibody alone or in combination with TMZ did not significantly enhance cell death (**Figure 11B**).

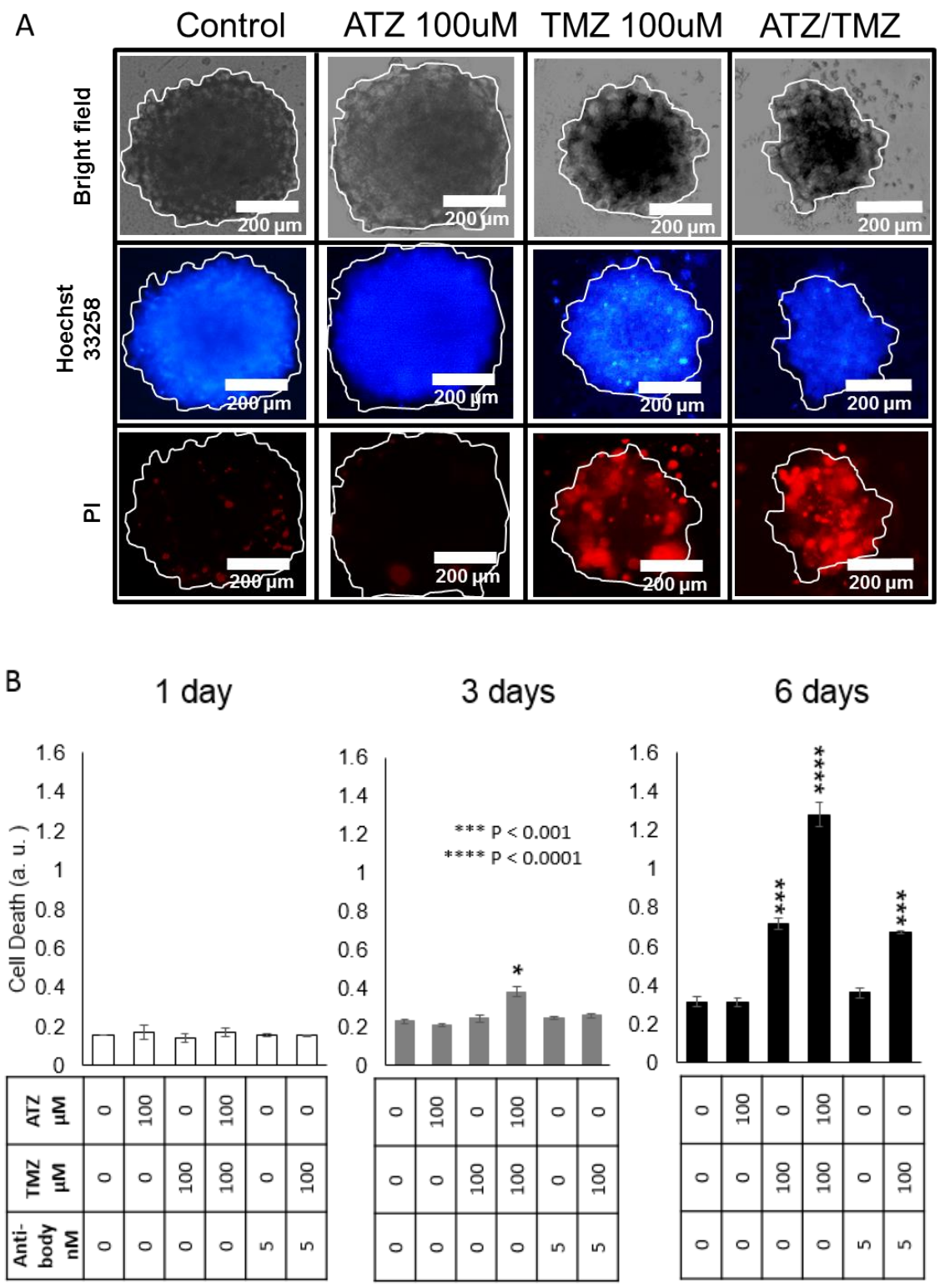

Figure 11. Combination therapy with CA IX inhibition and temozolomide treatment promotes cell death in glioblastoma spheroids.

(A) Morphological changes in U251N spheroids upon treatment with ATZ and TMZ (6 days). U251N spheroids (5K) were developed in a 96-well plate coated with 2% agarose (Invitrogen) in serum-deprived DMEM solution. Spheroids were seeded and maintained in filtered (0.22 µm) complete DMEM medium for four days before drug treatment with ATZ (100 uM), anti-CA IX antibody (5 nM), TMZ (100 uM) and with their combination for 1, 3 and 6 days. PI and Hoechst 33342 fluorescent dyes were added 4h prior to measurements. Following treatment, individual spheroids were imaged using a fluorescent microscope. (B) Enhancement of cell death upon combinatory treatments with ATZ and TMZ. Following treatments, PI and Hoechst 33342 fluorescent dyes were added 4h prior to measurements. Spheroids were then carefully transferred onto a microscope slide using a pipette, and flattened under a coverslip. Imaging after flattening of the spheroids was conducted using fluorescence microscope, and fluorescence intensity was quantified using ImageJ software. The ordinate shows the relative PI to Hoechst-33342 fluorescent intensity. The abscissa shows the concentration of the drugs as indicated. Average values and S.E.Ms. are reported for five measurements which were repeated in at least two to five independent experiments. Statistically significant differences from control were calculated using a t-test and are indicated by * ($p<0.05$), *** ($p<0.001$) and **** ($p<0.0001$).

3.3. Mechanisms of cell death through CA IX inhibition

Having seen the effect of CA IX inhibition by ATZ in combination with TMZ on the GBM cell viability in both monolayers and spheroids, we investigated the changes in some of cell death markers. Since the changes in GBM viability were most remarkable after 6 days, the cells were collected and analyzed for the biomarker analysis. We hypothesized that caspase-3, an established marker of apoptosis, is activated by the combinatory treatments with ATZ and TMZ in both 2D and 3D models. Caspase-3 activity was measured using a fluorescent based caspase-3 assay kit (refer to material and method). The principle of this assay is the cleavage of the caspase-3 substrate (Z-DEVD–R110 substrate) by activated caspase-3 (**Figure 12A**).

Caspase-3 activity was significantly increased with ATZ treatment of GBM cells in monolayers under hypoxic conditions ($CoCl_2$) but not in control cells without hypoxic or hypoxic cells in the absence of ATZ ($p<0.0001$ and $p<0.01$ respectively) (**Figure 12B**). In the spheroids, even though ATZ treatment alone did not significantly change caspase-3 activity, when it was combined with TMZ caspase-3 activity was significantly increased after 6 days treatment (**Figure 12C**).

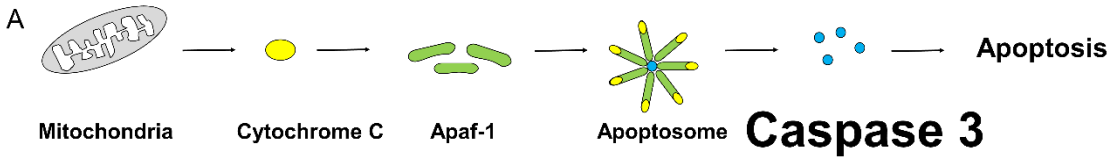

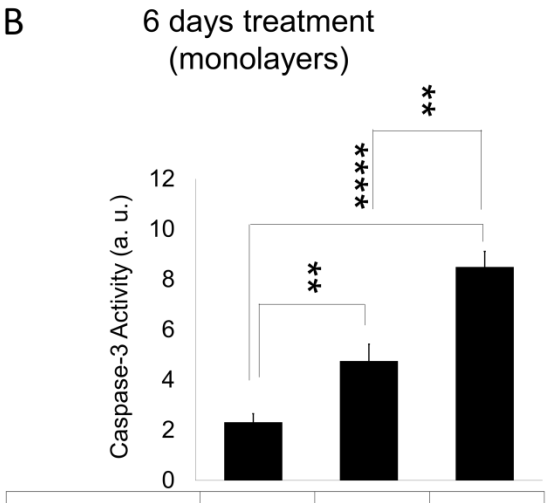

$CoCl_2$ µM	0	50	50
ATZ µM	0	0	100
TMZ µM	0	0	100

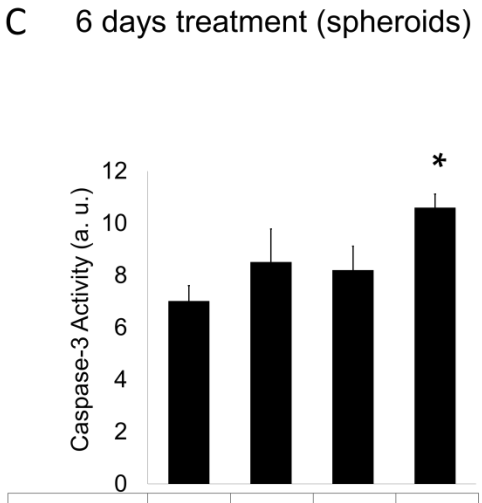

ATZ µM	0	100	0	100
TMZ µM	0	0	100	100

Figure 12. Caspase-3 activity increases in U251N glioblastoma cells upon combinatory treatment with ATZ and TMZ increases.

(A) The steps in caspase-3 activation leading to apoptotic cell death is illustrated. Reproduced with permission of Company of Biologists Ltd. in the format Republish in a

thesis/dissertation via Copyright Clearance Center, Journal of cell science by COMPANY OF BIOLOGISTS (Dewson & Kluck, 2009). (B) Significant increase in caspase-3 activity upon 6 days treatment with ATZ and TMZ. U251N monolayer were grown (300000 and 100000 cells for 1 and 6 days treatments respectively) in 6-well-plates in serum containing DMEM for 24 hours. Cells were then treated with either no treatment (control) or $CoCl_2$ (50 μM) for 24 hours to induce hypoxia. Then treatments were added as following: no treatment, ATZ (100 μM) and TMZ (100 μM) concomitant treatment for 6 days. Following the treatments, the cells were collected and were either counted or centrifuged at 11000 g for 4 minutes. (C) U251N spheroids (5K) were developed in a 96-well plate coated with 2% agarose in serum-deprived DMEM solution. They were seeded and maintained in filtered (0.22 μm) complete DMEM medium for four days before drug treatment with ATZ (100 μM), TMZ (100 μM), and with their combination (concomitantly) for 6 days. Following the treatments, spheroids were collected and centrifuged. EnzCheck Caspase-3 assay kit #2 was then used for both monolayers and spheroids as following: cells were lysed and then centrifuged. Then, 50 μl of the supernatant from each treatment was added to a black 96-well-plate followed by addition of the reaction buffer and incubation for 30 minutes. The fluorescence signals (excitation/emission ~496/520 nm) were then measured by a spectrofluorometer (FLUOstar OPTIMA) (for full detail refer to the materials and method). The fluorescent signals (caspase-3 activity) were then normalized to the cell number and presented as above on the ordinate. The abscissa shows the drug concentrations as indicated. The results are representative of at least two independent experiments. Statistically significant differences from control were calculated using a t-test and are indicated by * ($p<0.05$), ** ($p<0.01$) and **** ($p<0.0001$).

To further investigate the mechanism of cell death, we measured BAX, a biomarker of apoptosis upstream of caspase-3. U251N spheroids 4 days old were treated with ATZ, TMZ and their combination. Spheroids were then collected and lysed. The total cell lysate was immunoblotted for BAX expression. ATZ alone did not significantly change BAX expression, though TMZ did enhance BAX expression significantly (1.3 ± 0.2

p<0.05). Nevertheless, the highest BAX expression was measured for ATZ and TMZ combinatory treatment (1.8±0.5 (p<0.05) (**Figure 13B**).

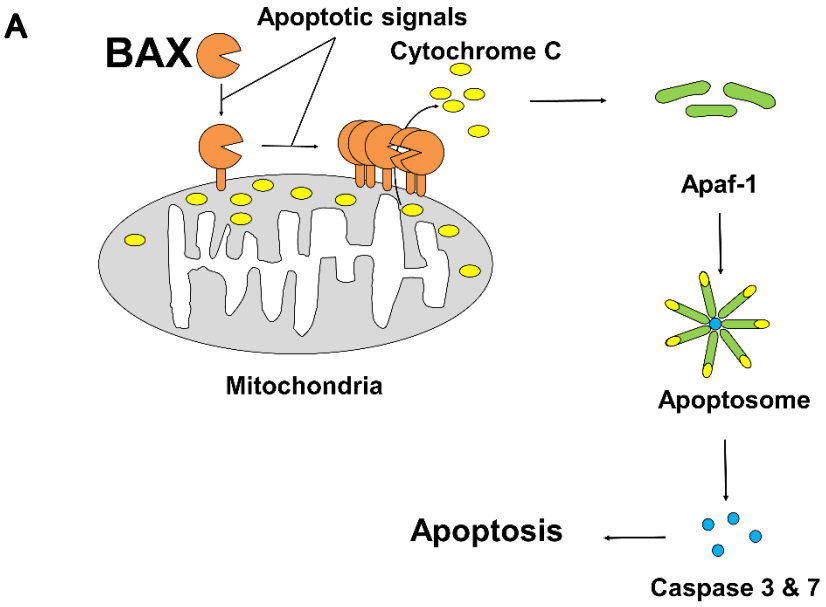

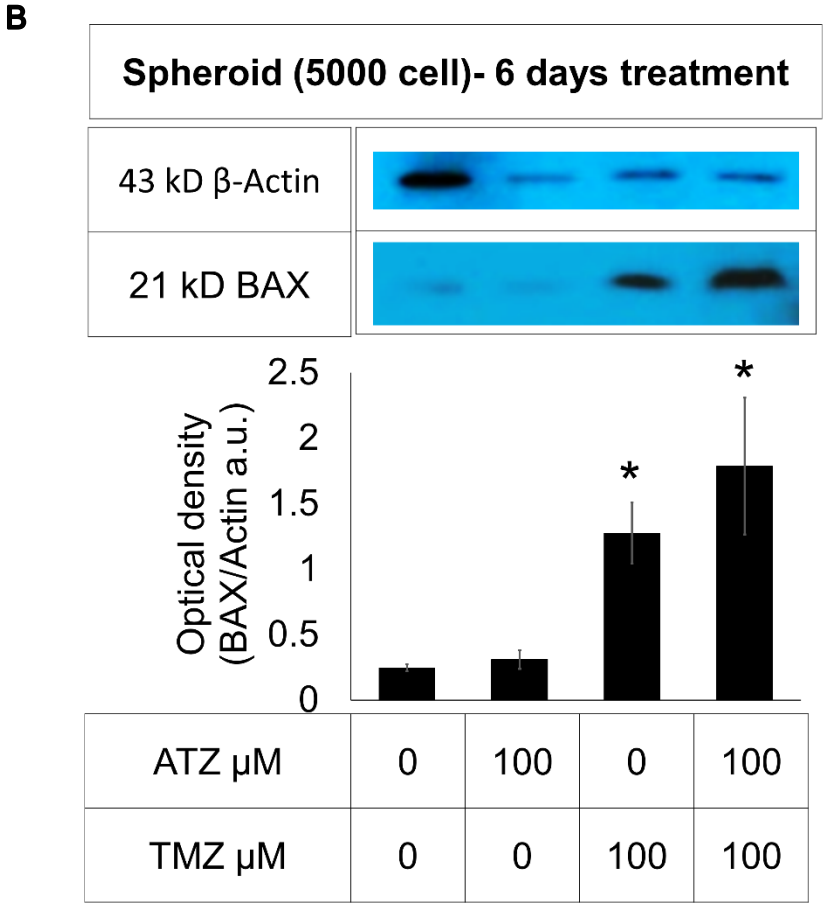

Figure 13. BAX expression in GBM spheroids is enhanced upon ATZ and TMZ combinatory treatment.

(A) BAX expression and Baxosome formation leading to apoptotic cell death is illustrated. Reproduced with permission of Company of Biologists Ltd. in the format Republish in a thesis/dissertation via Copyright Clearance Center, Journal of cell science by COMPANY OF BIOLOGISTS (Dewson & Kluck, 2009). (B) Significant increase in BAX expression upon treatment with ATZ and TMZ. U251 spheroids were developed as described previously. They were then treated with ATZ (100 μM), TMZ (100 μM) and with their combination for 6 days. Following the treatment spheroids were picked up by a pipette, centrifuged and lysed. Total cell lysate was collected and immunoblotted for BAX. The Level of expression of BAX is presented as the optical density of the bands over their respective actin band, protein loading control (10 μg), on the ordinate. The abscissa shows the concentrations of the drugs as indicated. The results are representative of at least three independent experiments. Statistically significant differences from control were calculated using a t-test and are indicated by * ($p<0.05$).

3.4. Nano-delivery of ATZ in micelles

Although the combination treatment with ATZ did increase cell death at long term treatments, ATZ has a low solubility in water and it degrades upon exposure to light, water and blood. Therefore, we hypothesized that the encapsulation of the ATZ into the nano-carriers such as micelles, will enhance its therapeutic effectiveness.

To prepare the ATZ micelles, commercially available co-polymer polyethylene glycole-poly lactic poly glycolic acid (PEG-PLGA; PEG 2,000 g/mol; PLGA 4,000 g/mol) and ATZ were dissolved in tetrahydrofurane (THF) with sonication to obtain a clear solution. They were then added drop-wise to an equal amount of water followed by removal of THF by vacuum. The excess non-encapsulated ATZ was then removed by centrifugation (10 min, 1000 g)-(**Figure 14A**). The prepared micelles were then characterized by asymmetrical flow field-flow fractionation (for full detail refer to materials and method) (**Figure 14B**) to determine their sizes. Also the concentration of

the ATZ in the micelles was calculated using the total ATZ minus the non-encapsulated ATZ.

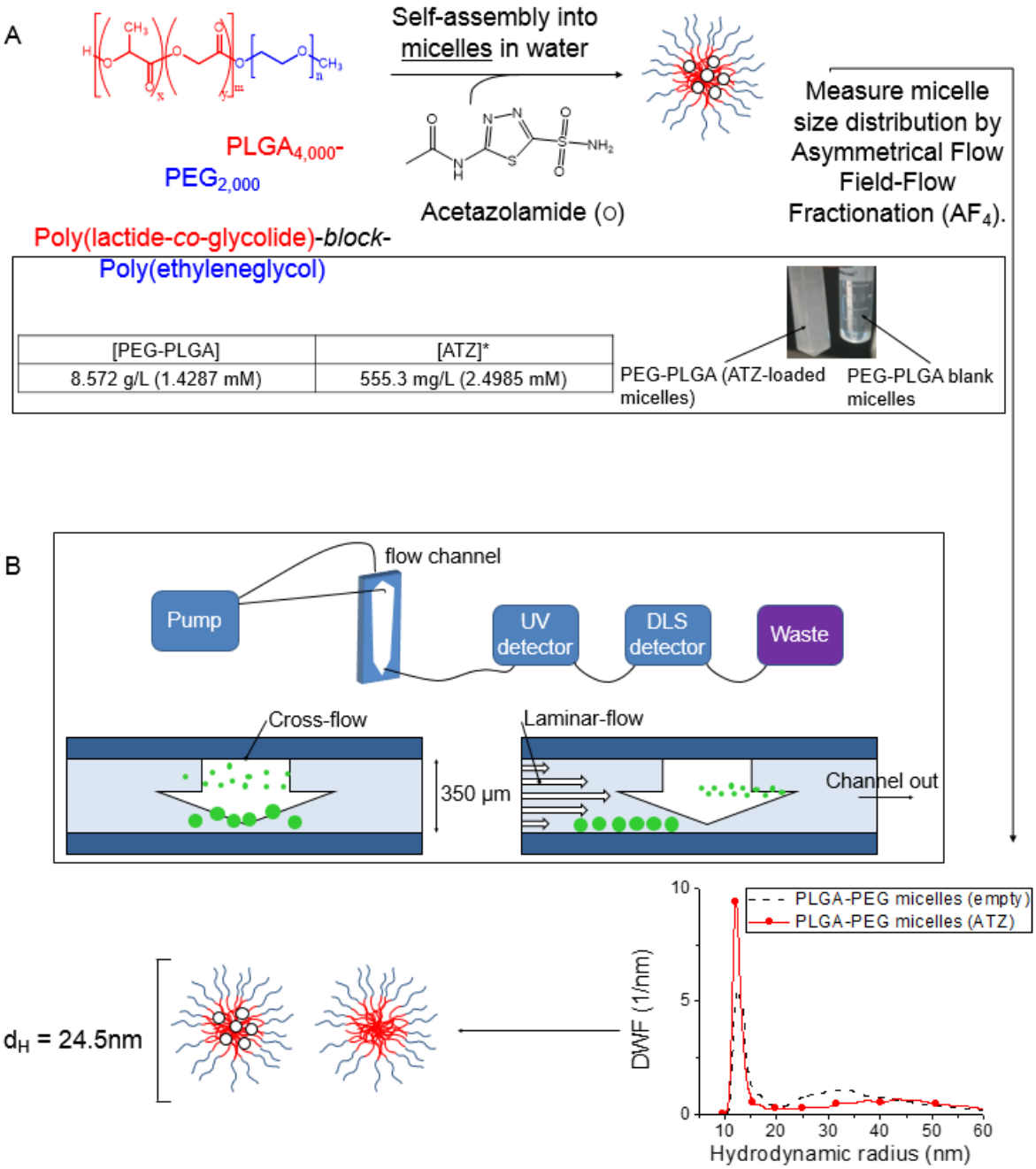

Figure 14. Preparation and characterization of ATZ-micelles.

(A) Loading of the spheroids with ATZ is illustrated. ATZ-loaded micelles were prepared by dissolving PEG-PLGA and ATZ in THF with sonication to obtain a clear solution. An equal volume of water was placed in a vial with a magnetic stirrer. The THF solution

containing polymer alone or a mix of polymer-drug was then added into the water. Then the THF was removed in vacuum. The excess non-encapsulated ATZ was removed by centrifugation (10 min, 1000 g), and its mass was determined after freeze-drying to remove any trace of water. (B) The empty and ATZ-loaded micelles are similar in size. The size of the blank and ATZ-loaded micelles was determined by asymmetrical flow field-flow fractionation (AF4, Dualtec, Wyatt Corporation, Santa Barbara, CA, USA) coupled to a UV-Vis detector set at 250 nm and a dynamic light scattering detector (DLS). The nanoparticles injected in the AF4 elute out of the instrument depending on their physical sizes. Smaller particles elute early followed by larger ones. Size distribution of ATZ-loaded and blank micelles of PEG-PLGA is shown in the fractogram illustrated on the bottom right (DWF=differential weight fraction). The abscissa shows the hydrodynamic radius.

Next, the prepared ATZ micelles were used for treatment of the spheroids for 1-6 days, alone and in combination with TMZ. Much to our surprise, the cell death caused by encapsulated ATZ alone (0.70$\pm$0.01 a.u.) or in combination with TMZ (0.73$\pm$0.02 a.u.) was highly significant after even one day treatment ($p<0.0001$). Cell death was further enhanced after 3 days of treatment while cell death caused by ATZ micelles combined with TMZ after 6 days treatment caused the most significant cell death (1.00$\pm$0.08 a.u., $p<0.0001$) compared to 1 and 3 days treatment (**Figure 15B**).

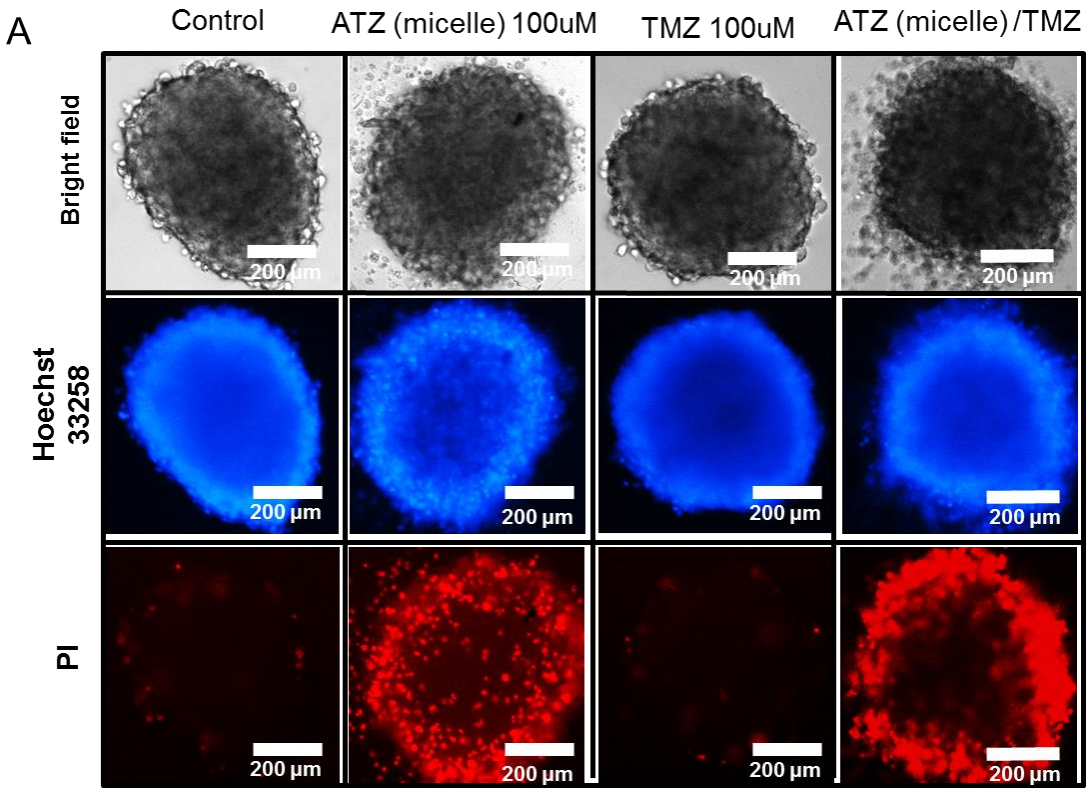
A
Control
ATZ (micelle) 100uM
TMZ 100uM
ATZ (micelle) /TMZ
Bright field
Hoechst 33258
PI
200 µm

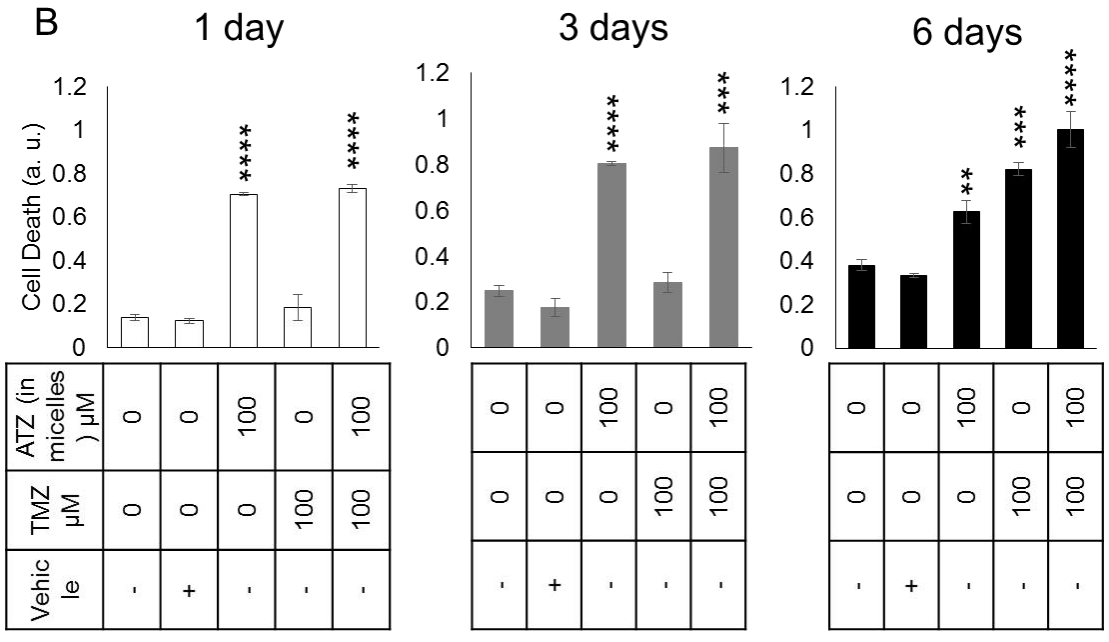
B
1 day
3 days
6 days
Cell Death (a. u.)
1.2
1
0.8
0.6
0.4
0.2
0
**
***
****
ATZ (in micelles) µM
TMZ µM
Vehicle
0
100
-
+

Figure 15. Cell death caused by ATZ treatment significantly increases when delivered in micelles.

(A) Morphological changes in U251N spheroids upon treatment with ATZ micelles (1 day). U251N spheroids (5K) were developed as described previously followed by drug treatments with the vehicle, ATZ micelles (100 uM), TMZ (100 uM) and with their combination for 1, 3 and 6 days. PI and Hoechst 33342 fluorescent dyes were added 4h prior to measurements. Following treatment, individual spheroids were imaged using a fluorescent microscope. (B) Significant cell death caused by ATZ-micelles. Following treatments, PI and Hoechst 33342 fluorescent dyes were added 4h prior to measurements. Spheroids were then carefully transferred onto a microscope slide using a pipette, and flattened under a coverslip. Imaging after flattening of the spheroids was conducted using fluorescence microscope, and fluorescence intensity was quantified using ImageJ software. The ordinate shows the relative PI to Hoechst-33342 fluorescent intensity. The abscissa shows the concentration of the drugs as indicated. Average values and S.E.Ms. are reported for five measurements which were repeated in at least two to five independent experiments. Statistically significant differences from control were calculated using a t-test and are indicated by ** ($p<0.01$), *** ($p<0.001$) and **** ($p<0.0001$).

3.5. CA IX expression in the BTSCs

In our previous models, the GBM monolayers and spheroids, we established the importance of CA IX expression and the effect of its inhibition on GBM cell viability. BTSCs, postulated to be responsible for recurrence of GBM, form neurospheres which have a supposedly hypoxic core (**Figure 16A**). Therefore, we hypothesized that CA IX is expressed in these cells.

Several types of BTSC were cultured in complete Neurocult-NS-A proliferation medium for 6-10 days. Then they were spun down and lysed. The total cell lysate was separated using denaturing conditions and transferred to the cellulose membrane immunoblotted for CA IX expression. CA IX was expressed in all of the BTSCs (6-10 days) in our experiment. CA IX expression was significantly higher in 48EF (10 days) and OPK49

cells compared to U251N spheroids (10 days) (5.2±0.2, $p<0.01$ and 3.3±0.4, $p<0.05$ respectively) (**Figure 16B**).

A

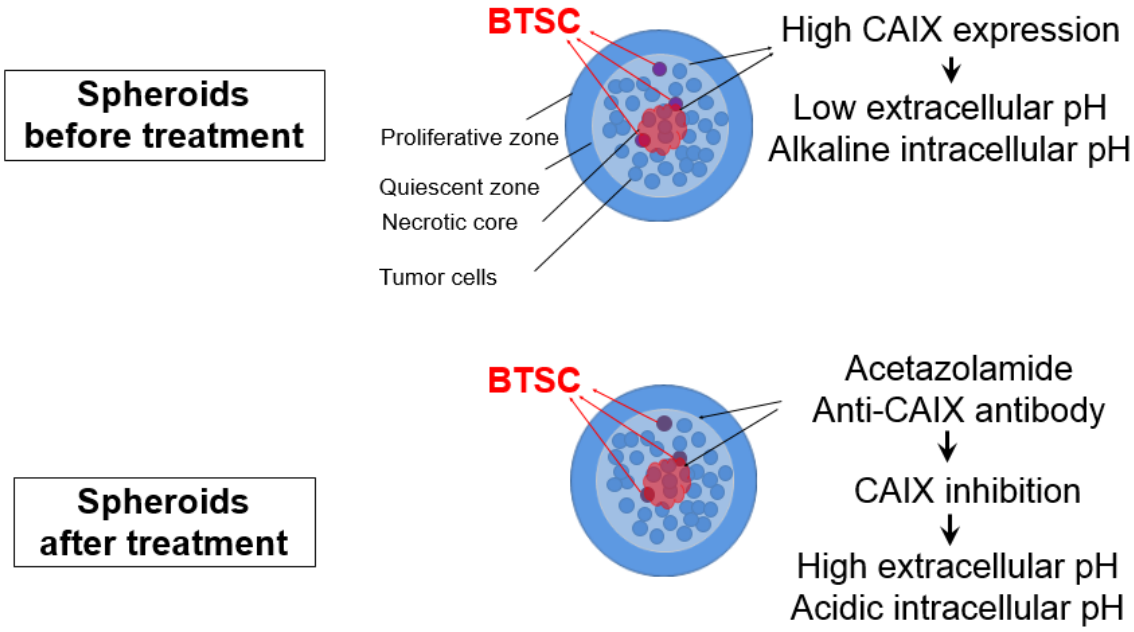

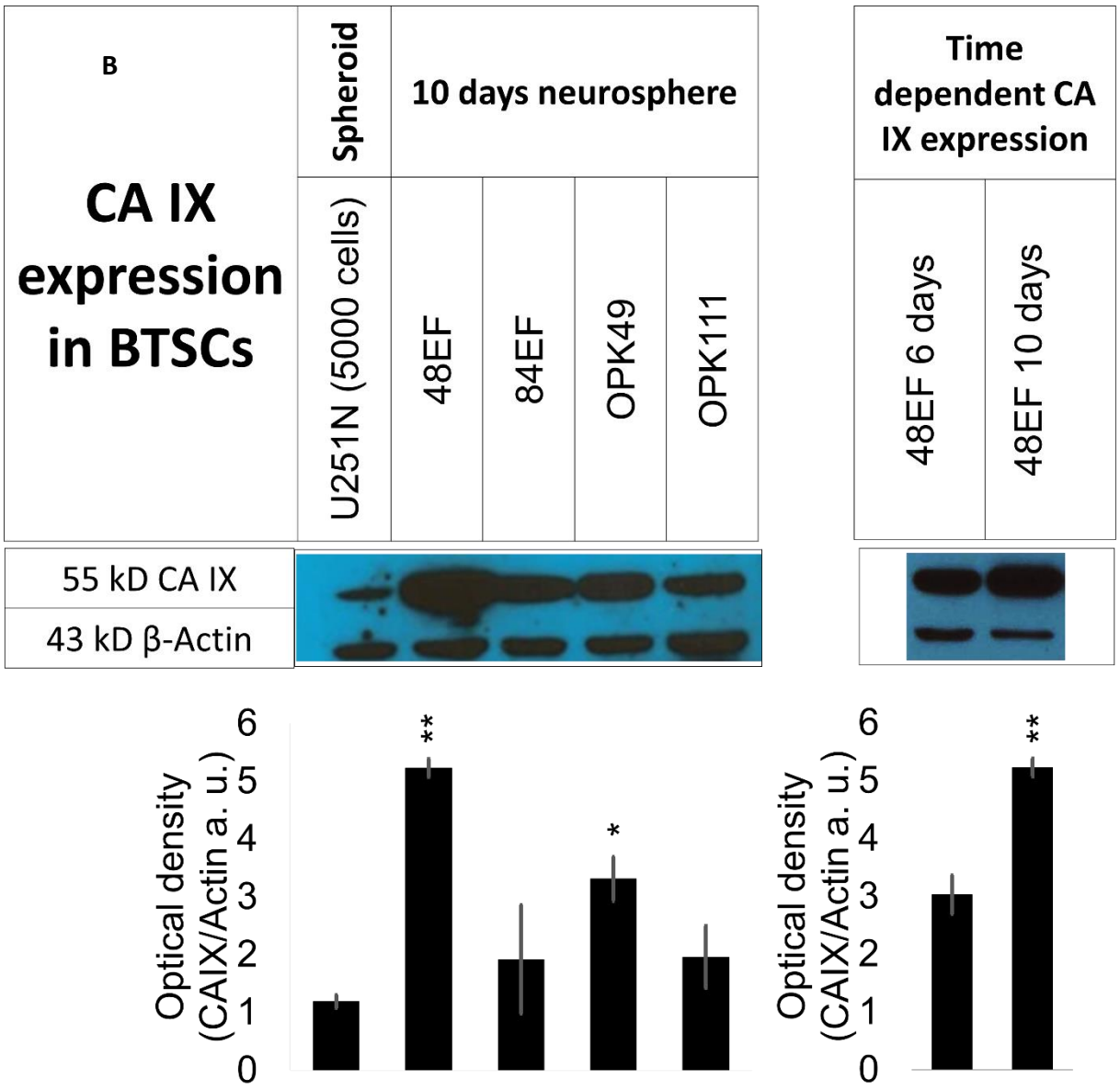

Figure 16. CA IX is highly expressed in the BTSCs in a time dependent manner.

(A) CA IX inhibition in the spheroids is illustrated. (B) CA IX is highly expressed in BTSCs. Cells were seeded at a concentration of 200k cells per flask in complete Neurocult-NS-A proliferation Medium and incubated for 6-10 days at 37^{o}C. Then they were collected, pelleted, washed with PBS and lysed. Total cell lysate was collected and immunoblotted for CA IX. The Level of expression of CA IX is presented as the optical density of the bands over their respective actin band, the protein loading control (10 μg), on the ordinate. The abscissa shows the neurosphere's age and type as

indicated. The results are representative of at least two independent experiments. Statistically significant differences from control were calculated using a t-test and are indicated by * ($p<0.05$) and ** ($p<0.01$).

Next, we hypothesized that the inhibition of CA IX with ATZ alone or ATZ delivered in nano-carriers (micelles) will enhance cell death in BTSCs. Although one day treatment with ATZ alone did not significantly change the morphology of the neuropheres, when delivered by micelles, it distorted the spheroids shape and led to detachment of the cell (**Figure 17A**), indicated by red arrows. Moreover, the assessment of the mitochondrial metabolic activity using the XTT assay, indicative of no significant decrease in cell viability by ATZ alone. In contrast, when ATZ was delivered in micelles it resulted in complete elimination of the cells when delivered in micelles ($p<0.05$) (**Figure 17B**). Similar to U251N spheroids, cell death of BTSC caused by ATZ micelles was dose dependent (data not shown).

A

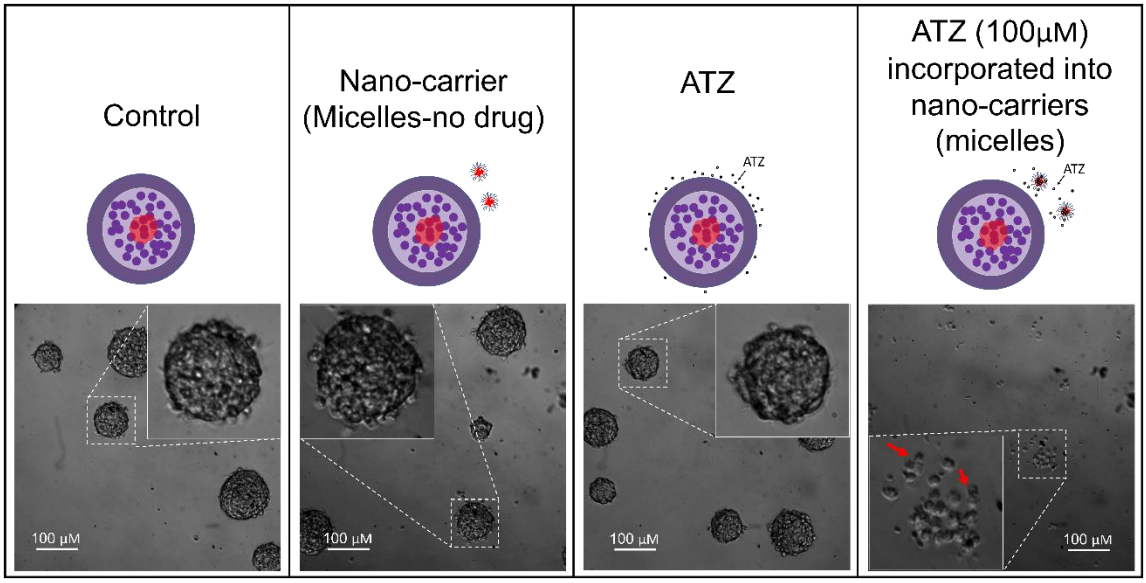

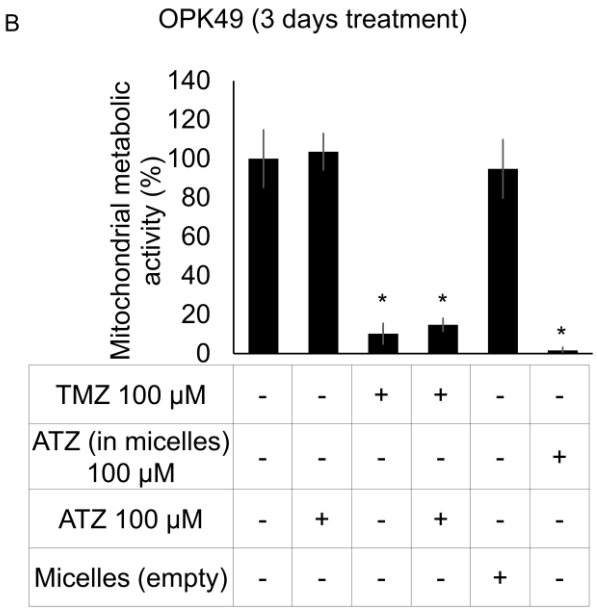

Figure 17. Inhibition of CA IX by ATZ micelles compromises BTSCs viability.

(A) Dispersion of cell in the neurospheres by ATZ micelles. Modes of delivery of the drugs to the brain tumor stem neurospheres are illustrated. BTSCs were plated in 6 well plates at a concentration of 200 000 cells/well and were grown for 24 followed by treatments with the vehicles, ATZ (100 µM) and ATZ micelles (100 µM) for 72 hours as indicated. Then they were imaged using bright field microscopy. The red arrows show the detached cells. (C) Significant reduction in BTSCs viability upon ATZ micelles treatment. BTSC were plated at 10 000 cells/well in 96 well overnight in culture media. Drugs were added to their final concentrations in a final volume of 200 µl and kept for 72 hours at 37°C. 50µl of XTT was prepared and was added and further incubated for 2 hours at 37°C. The absorbance at 490 nM was measured and expressed in percentage of mitochondrial metabolic activity on the ordinate. The abscissa shows the drug treatments as indicated. The results are representative of at least two independent experiments. Statistically significant differences from control were calculated using a t-test and are indicated by * ($p<0.05$).

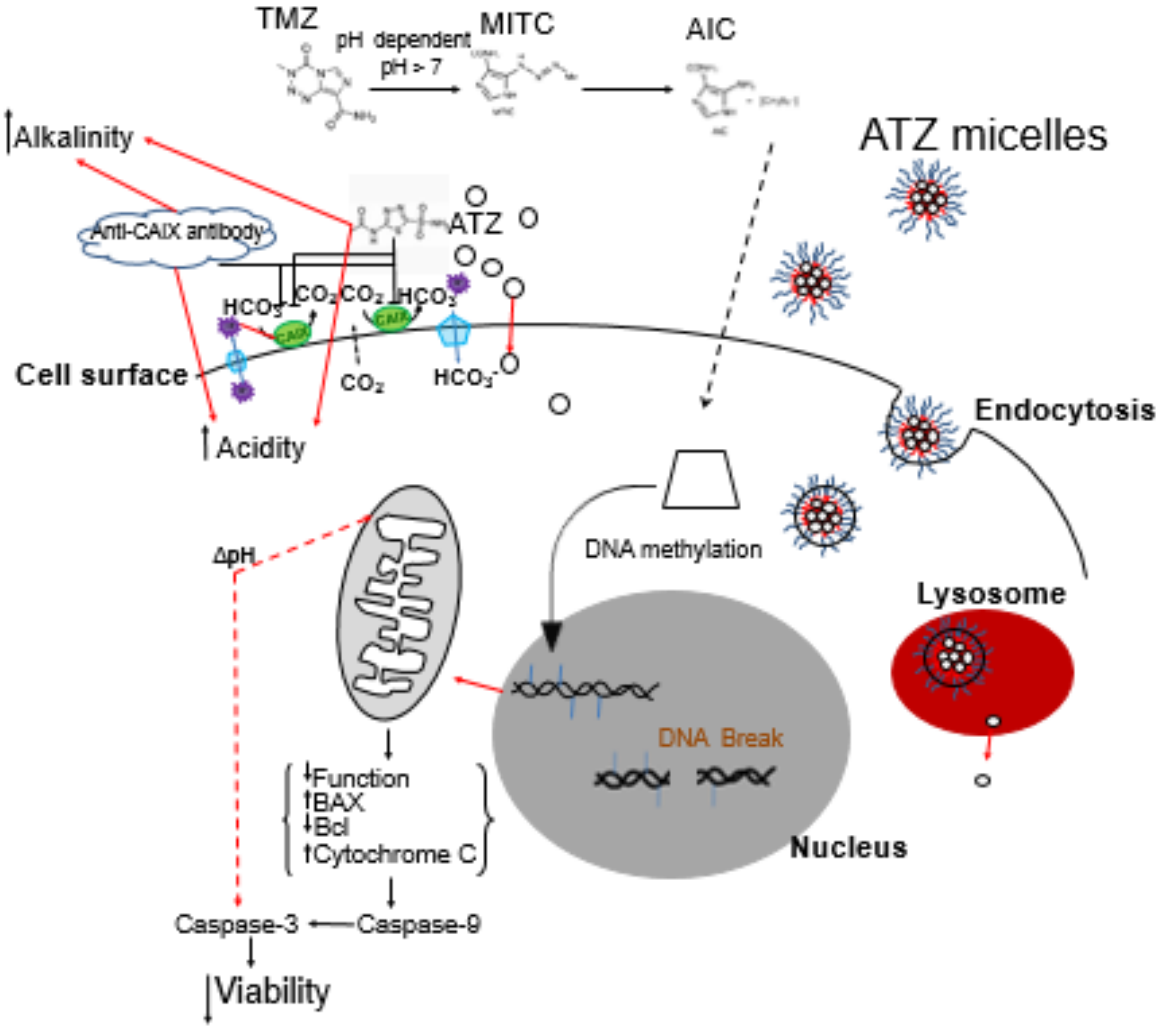

Figure 18. Disruption of signal transduction pathways in glioblastoma exposed to combined treatment inhibiting CA IX and binding to nuclear DNA.

TMZ is a prodrug which needs to be cleaved to its active form. The cleavage of TMZ to MITC is entirely pH dependent. CA IX inhibition leads to an increase in the extracellular pH of the cell which can facilitate TMZ cleavage into its active form. On the other hand, CA IX inhibition can lead to a decrease in the intracellular pH of the cells leading to an increase in the cell proliferation and consequent increase in DNA damage by TMZ. Also, the decreased intracellular pH can increase caspase-3 activity leading to an increase in apoptosis and cell death.

Chapter 4: Discussions

4.1. Expanding the role of CA IX as a marker of hypoxia in GBM to a therapeutic target

In this research, we sought to evaluate whether *in-vitro* models of GBM, using established cell lines and most significantly, Brain Tumour Stem Cells (BTSC), could be used to validate CAIX as a therapeutic target in GBM. Furthermore, we sought to find whether the action of the only approved chemotherapeutic agent for GBM, TMZ, could be augmented by the inhibition of CA IX and by evaluating its mechanisms of cell death in glioma cells.

4.1.1. CA IX expression and hypoxia

CA IX is a transmembrane enzyme which catalyzes the reversible conversion of carbon dioxide to carbonic acid ($CO_2 + H_2O$ to HCO_2^- and H^+). The expression of CA IX is restricted in normal cells while it is highly overexpressed in hypoxic tumors and particularly in the case of GBM (Proescholdt et al., 2012). CA IX is, a transmembrane protein involved in pH homeostasis in hypoxic tumors (**Figure 7**) (Kaluz et al., 2009; McDonald et al., 2012).

In tumours, the oxygen availability plummets, mainly due to the rapid cellular proliferation and the abnormal structure and function of the tumor blood vessels (Vaupel, Mayer, & Hockel, 2004). The occurrence of intratumoral hypoxia increases as the distance from the nearest blood vessel increases. The diffusional distance of oxygen is about 100–200 μm, while the disorganized vascular networks in tumours lead to intercapillary distances which very commonly exceed the oxygen diffusion distance (Sorg, Hardee, Agarwal, Moeller, & Dewhirst, 2008). Due to the Warburg effect, tumor cells use high levels of aerobic glycolysis (Warburg, Wind, & Negelein, 1927). More importantly, under hypoxic conditions where cells are obliged to use anaerobic glycolysis as their main source of energy (the Pasteur effect) (Porter, 1961), glycolysis is further augmented. Such metabolism of glucose leads to accumulation of high lactic acid load and drastic changes in intracellular (pH_i) and extracellular (pH_e) pH, which are mainly regulated by CA IX (Parks, Chiche, & Pouyssegur, 2011; Sonveaux et al., 2008).

Among all human α-carbonic anhydrases, CA IX has the highest catalytic activity and the exposure of its catalytic domain to the extracellular domain allows its contribution to the pH_i and pH_e (exchange). This occurs through catalytic reaction of water and CO_2 and production of bicarbonate which is then transported into the cell (e.g. through Cl^- /bicarbonate exchanger) and export protons to the stroma (Introduction, **Figure 5**)(Swietach, Vaughan-Jones, & Harris, 2007; Wingo, Tu, Laipis, & Silverman, 2001).

The poor oxygenation status of tumors, particularly in high grade gliomas, plays a critical role in the poor tumor response to radiation and many chemotherapeutics (Bernsen et al., 2000; Bussink et al., 1999).

One of the main reasons for the malignant progression and the high resistance of the hypoxic tumors to therapeutics is the substantial changes in the gene regulations due to the oxygenation status of the tumors (Hockel et al., 1996). The transcriptional activity of the hypoxia inducible factors (HIF1 and HIF2) plays the most important role with regards to cancer cell adaptation to the hypoxic environment (Gilkes, Semenza, & Wirtz, 2014). Under hypoxic conditions a transcription factor HIF1α is stabilized and transported to the nucleus. Nuclear HIF1α initiates transcription of hypoxia related genes of which CA IX, is highly upregulated. A myriad of studies have demonstrated CA IX plays critical roles in the tumor cells, including cell survival and proliferation, stem cell phenotype maintenance (Lock et al., 2013), epithelial-mesenchymal transition (EMT) in carcinoma cells (Fiaschi et al., 2013), invasion and metastasis. Extensive experimental studies have correlated CA IX expression in hypoxic tumors with their resistance to radiotherapy and to many chemotherapeutics (Potter & Harris, 2004; Proescholdt et al., 2012).

4.2. *In vitro* investigations to study therapeutic interventions against CA IX in GBM

In order to study the role of CA IX and the effect of its inhibition in the context of GBM several different *in vitro* model systems have been explored: monolayers (2D culture), cancer cell spheroids (3D culture) and brain tumour stem cell neurospheres (3D culture). *In vivo* GBM models have been used for the screening of candidate anticancer agents, but the molecular mechanisms cannot be easily determined under such

conditions because of interferences from different systems; endocrine and other systems. (Rao, Lannutti, Viapiano, Sarkar, & Winter, 2014).

Studying hypoxic conditions in monolayer cell cultures is not straight forward. CA IX expression can be upregulated by chemical reagents such as $CoCl_2$ or by CA IX gene transfection or the use of hypoxic chambers (Chen et al., 2005; Matsubara, Diresta, Kakunaga, Li, & Healey, 2013; Teppo et al., 2013). In our study, we have used $CoCl_2$ in GBM cell culture monolayers. In contrast to monolayers, in spheroids, the 3D cell culture models form an intrinsic hypoxic core which does not necessitate an artificial induction of hypoxia for CA IX expression (Results, **Figure 7A**).

4.2.1. Induction and suppression of CA IX in monolayers

In the monolayer cultures, exposure of U251N cells to $CoCl_2$ induced a chemical hypoxic state and resulted in a significant concentration-dependent increase in CA IX protein expression after 3 days. (Results, **Figure 7B**). Our results are in agreement with previous findings in several studies on different GBM cell lines including U251N (Said et al., 2013; Teppo et al., 2013). In the study by Said et al., it was shown that the CA IX expression is low to undetectable under normoxia in U251, U373 and GaMG GBM cell lines. However, under hypoxic conditions (0.1% O_2) CA IX is highly expressed in all of the aforementioned cell lines.

When the U251N monolayers were subjected to addition of ATZ, complete suppression of CA IX protein expression was also seen (Results, **Figure 7**). This unusual supplemental inhibitory mechanism relates to the intra-cellular presence of the inhibitor, something not achieved by molecular changes designed to keep the inhibitors in the extracellular milieu.

Having established the hypoxic monolayer models, we hypothesized that the inhibition of CA IX would enhance cell death. Therefore, we treated the hypoxic U251N monolayers with ATZ and the anti-CA IX antibody for different time periods (**Figure 8**). Neither the ATZ nor the antibody alone increased cell death under hypoxia. The combination of ATZ with TMZ caused a moderate, but significant increase in cell death compared to TMZ alone (14 ± 1 ($p<0.01$) and 20 ± 2 ($p<0.01$) respectively). CA IX

inhibition did not enhance cell killing, this is likely due to the buffering effect of the media, which is difficult to overcome in monolayers (Lou et al., 2011).

4.3. U251N spheroids as an improved *in-vitro* model of GBM

It is now widely established that tumor cell behaviour and signalling cascades are substantially different in 2D and 3D cultures (Cukierman, Pankov, Stevens, & Yamada, 2001; Yamada & Cukierman, 2007). 3D cultures mimic more closely the *in vivo* environment in many critical ways than 2D cultures (**Table 4**) (Yamada & Cukierman, 2007).

Biological function	2D versus 3D
Gene expression	Cells in 2D versus 3D often have different patterns of gene expression (S. Li et al., 2003)
Growth	3D matrix-dependent regulation of cell growth (O'Brien, Zegers, & Mostov, 2002)
Motility	Altered single and collective cell motility patterns in 3D matrices (Fisher et al., 2006)
Differentiation	3D matrix-induced cell differentiation (Engler, Sen, Sweeney, & Discher, 2006)
Morphogenesis	3D matrix-induced vessel sprouting and gland branching (O'Brien et al., 2002)

Table 4. 3D behaviour cell behaviour and signalling.

Adapted from (Yamada & Cukierman, 2007) with permission from Elsevier.

One of the important characteristics of the 3D models (spheroids) is the formation of a hypoxic core within the spheroids. Our results clearly show a significant CA IX expression (**Figure 10A** and **B**) as a result of hypoxia. Thus we hypothesized that the

expression of CA IX would enhance as the spheroids grow bigger in size with time (**Figure 9A**). Similarly spheroids formed from the initially larger number of cells attain hypoxic cores in a shorter time period (**Figure 9B**). As expected, CA IX expression significantly increased in a time and size dependent manner (**Figure 10A** and **B**). Consistent with our results, studies by Imamura et al. also showed the presence of hypoxia in the 3D multicellular breast cancer spheroids (three cell lines: BT-549, BT-474 and T-47D) (Imamura et al., 2015).

4.3.1. Inhibition of CA IX in Spheroids

Considering the critical role of the CA IX in spheroid growth and survival, we anticipated that the inhibition of CA IX would enhance cell death in U251N spheroids in the presence or absence of TMZ. Spheroids exposed to the inhibitors of CA IX (ATZ and the antibody) alone did not reveal a significant increase in cell death. Similar to our findings, studies by Das et al. confirmed a minor increase in cell death upon ATZ treatment in the T98G and U87MG GBM cell lines (Das, Banik, & Ray, 2008).

Next, we tested the TMZ and ATZ drug combination in U251N spheroids. As opposed to the moderate increase in cell death in monolayers by ATZ and TMZ combination, a highly significant increase in cell death was observed in the spheroids after 6 days of treatment compared to TMZ treatment alone. The highly enhanced cell death in the spheroids upon CA IX inhibition combined with TMZ treatment can be due to the consequent increase in the extracellular pH creating an alkaline microenvironment for TMZ activation facilitating its cell entry (H. S. Friedman et al., 2000). Additionally the CA IX inhibition would also lead to the acidification of the intracellular pH of the cells in the spheroids leading to sensitization of the cell to TMZ treatment (Swietach, Hulikova, Vaughan-Jones, & Harris, 2010).

4.4. Model systems using BTSC as an *in-vitro* model of GMB

Development of accurate models of cell populations that produces the heterogeneous population of cells within a tumor is an essential step for designing effective therapy. BTSC are slow-dividing, small population within a heterogeneous GBM which can recapitulate a whole tumor and differentiate into other specific GBM subpopulations (Auffinger, Spencer, Pytel, Ahmed, & Lesniak, 2015).

BTSC tend to preferentially reside within the hypoxic core of tumor mass (Persano, Rampazzo, Della Puppa, Pistollato, & Basso, 2011). Considering their preferential location, we anticipated that they express CA IX as one of the key enzymes expressed under hypoxia. Our results clearly showed highly significant expression of CA IX in several types of BTSC (**Figure 16B**). In fact, CA IX expression was significantly higher in 48EF and OPK49 BTSCs ($p<0.01$ and $p<0.05$) in comparison to GBM U251N cell line. Similar to GBM spheroids, the expression of CA IX in BTSC (EF48) was also significantly enhanced with time ($p<0.01$) (**Figure 16B**). Consistent with our findings, in a study by Daisuke Fujiwara et al., it was shown that the 3-D esophageal squamous carcinoma stem cell lines TE2 and TTn had a highly significant expression of CA IX in the 7 days old spheroids. The very high and specific expression of CA IX in the BTSC is an interesting finding which can be used as a therapeutic target for elimination and prevention of recurrences in GBM. The effect of CA IX inhibition alone or in combination with TMZ in BTSC is discussed in later sections.

4.5. Design and testing of CAIX inhibitors

Overexpression of CA IX in hypoxic tumors and the localization of the active moiety at the extracellular site allows for the use of functionality blocking antibodies and targeted delivery of anticancer therapeutics in immunoliposomes (Pickering & Larkin, 2015; Shinkai et al., 2001)

To modulate multiple functions of CA IX in solid tumors beyond pH control (Proescholdt et al., 2012), approaches have been used based on RNA interference (RNAi) (Ameres & Zamore, 2013; Radvak et al., 2013; Shin et al., 2011). In a study by Jérome Doyen et al., it was demonstrated that CA IX knock down by short-hairpin RNA-CA IX in LS174Tr cells reduced cell proliferation in both 2D and 3D cultures (Doyen, Parks, Marcie, Pouyssegur, & Chiche, 2012).

4.5.1. The sulfonamide drug classes

Among the CA inhibitor small-molecule drug classes, the sulfonamide- based compounds are the most utilized and the most potent (Aggarwal, Kondeti, & McKenna, 2013). Many laboratories have successfully designed small molecule inhibitors or antibodies to manipulate the function and expression of CA IX (illustrated in **Figure19**).

However, due to the conserved architecture of the active site among human CAs, some of the CA IX inhibitors display inhibition of other CAs (**Figure 19**).

The extracellular location of the CA IX active site has therefore been taken advantage of for more selective drug design (Aggarwal, Kondeti, & McKenna, 2013; Hilvo et al., 2008). Manipulations of the physiochemical properties of the sulfonamide CA inhibitors to make them impermeable to the plasma membrane, changes their selectivity and increases the CAIX functional inhibition. (**Figure 19 and Table 5**) (Aggarwal et al., 2013).

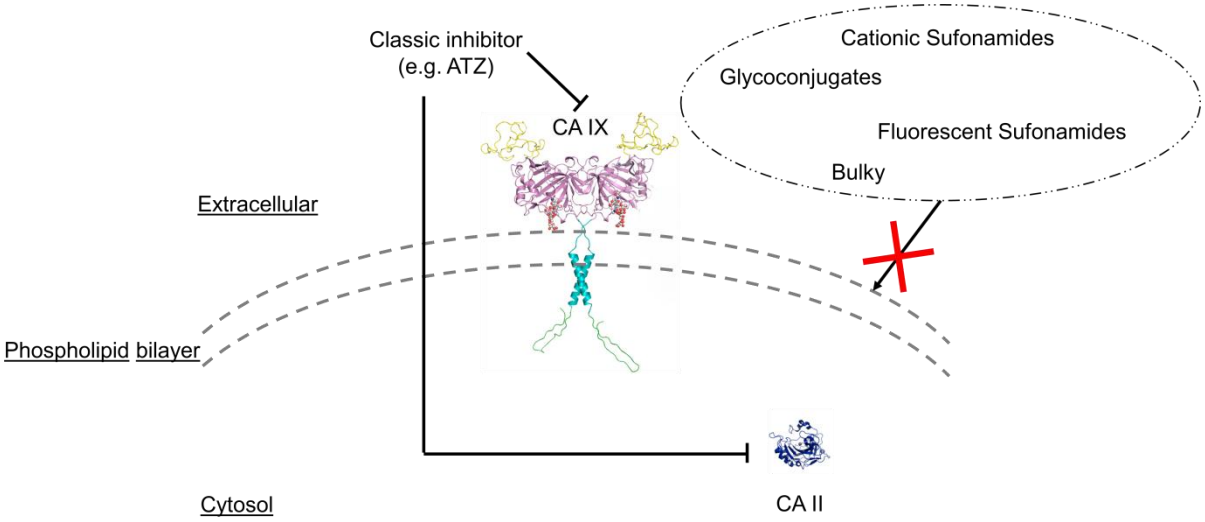

Figure 19. Specific and non-specific inhibition of CA IX.
Adapted from (Mahon, Pinard, & McKenna, 2015) with permission from Elsevier.

CA IX inhibitor	Mode of inhibition	Type
Albumin ATZ (Ahlskog, Dumelin, Trussel, Marlind, & Neri, 2009)	Small molecule inhibitor	Location specific
Glycoconjugated sulfamide (Moeker et al., 2014)	Small molecule inhibitor	Location specific
Coumarin derivatives (Grove, Gautheron, Plazonnet, & Sugrue, 1988)	Small molecule inhibitor	Prodrug like
CA IX directed immunolioposomes (Shinkai et al., 2001)	Antibody	Tumor specific with delivery system
RNAi technology and siRNA (Radvak et al., 2013)	Post-transcriptional gene silencing	CA IX knock down

Table 5. Current therapeutics and technologies used to target CA IX for the treatment of cancer.

Various types of potential prodrugs have been also developed for CA IX inhibition. Benzenesulfonamide, has a high affinity for CA IX (μM) and once it is unmasked its affinity for the enzyme increases by ~60 fold (Reich et al., 2012).

ATZ (ATZ), is a non-specific inhibitor of the CAs. However, it inhibits CA IX activity and it reduces its expression at the protein level, and surprisingly, at the mRNA level (Said et al., 2013) (**Figure 20**).

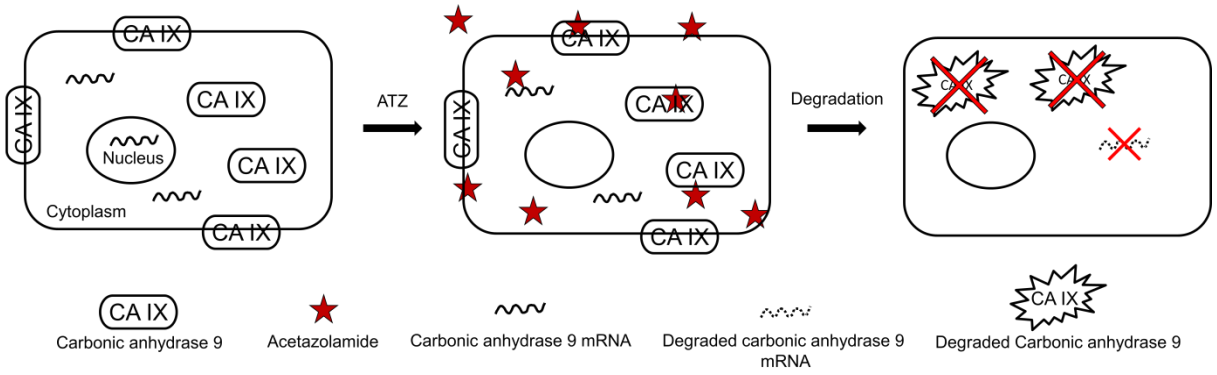

Figure 20. Degradation of CA IX by ATZ at the protein and the mRNA level. Adapted from (Said et al., 2013) with permission from Elsevier.

4.6. Nano-carriers for drugs for oncology and GBM

In the process of rational drug discovery, a massive number of compound libraries are screened for potential candidates that selectively act on a target of interest (Svenson & Chauhan, 2008). This step is followed by optimization of physicochemical properties of the potential candidates to provide the best pharmacokinetic profile followed by pre-clinical and clinical studies. A very high percentage (40%) of such newly developed active pharmaceutical ingredient (API) does not make it to the clinical testing due to poor pharmacokinetic properties (Svenson & Chauhan, 2008). In such circumstances, the engineered nano-carriers have become the novel solution to this issue.

We have further exploited this observation by the development of nano-formulations to enhance cellular penetration of this class of drug.

Liposomes, considered as the first generation nano-medicines, were discovered by Alec D Bangham which culminated in the market as one of the first nano-carriers (Bangham, 1968). Among the most successful nano-carriers to date (Dzieciuch et al., 2015; Lasic, 1996) are the second generation liposomes attached with polyethylene glycol (PEG) with reduced immunogenicity and slow rate of clearance (Abuchowski, McCoy, Palczuk, van Es, & Davis, 1977; Pasut & Veronese, 2012). Polymeric micelles are among the second and third generation nano-carriers which are quite advantageous with their flexible size range and sustained release kinetics. Of great interest are the biodegradable polylactide-co-glycolide (PLGA) nanoparticles which have been

approved by the US Food and Drug Administration (FDA) as safe and have been studied for the delivery of drugs to CNS (Costantino et al., 2005; Semete et al., 2010).

The polymeric micelles have been utilized for delivery of drugs to many types of cancers. In particular, polymeric micelles have been used in gliobalstoma mice models which were accompanied with significant improvement in the efficacy of the drugs (Kuroda et al., 2009; A. J. Li et al., 2015). Polymeric micelles developed by Kuroda et al. were used for the delivery of SN-38 to orthotopic GBM xenografts in nude mice and compared to CPT11 which is a prodrug. The tumor size reduction was significantly higher (up to 6 times) with the micellar formulation while the change in body weight was 10% less with micellar formulation suggesting a better and higher tolerance of the micellar formulation compared to the prodrug alone (Kuroda et al., 2009; A. J. Li et al., 2015).

Having seen the effectiveness of the combination treatment with ATZ and TMZ in our models, and knowing the low solubility of ATZ, and its susceptibility to the light and water, we wanted to see if the encapsulation of ATZ into the micelles would enhance its effectiveness in the 3D models (spheroids and neurospheres). As opposed to the free ATZ which did not affect cell viability after one day (**Figure 11B**), the ATZ micelles caused a significant increase in cell death even after one day treatment in U251N spheroids (**Figure 14B**). Similar to U251N spheroids, the OPK49 BTSC viability was not significantly reduced by free ATZ while the ATZ micelles completely eradicated the cells after 3 days of treatment ($p < 0.05$) (**Figure 17B**). As illustrated in **Figure 18**, the enhanced effectiveness of ATZ micelles is proposed to be due to several factors including: firstly, the release kinetics of ATZ from the micelles are such that ATZ is slowly released until the micelles are completely empty and disintegrated. In this way ATZ is constantly available for longer periods of time. Secondly, as opposed to free ATZ which can diffuse in and out of the cells, once the ATZ micelles are internalized they slowly release their cargo leading to constant presence of ATZ in the cells. Thirdly, ATZ is not a hydrophilic molecule and can form aggregates and precipitate while when it is encapsulated in the micelles, such issue would not occur. Finally the ATZ in the media

can get degraded over time losing its therapeutic effect while micelles can protect them from rapid degradation.

The observation of significant enhancement in cell death by ATZ micelles in both GBM and BTSC is an interesting observation which necessitates *in vivo* studies. The PEGylated micelles have been previously used for the delivery of TMZ to the brain using transferrin as a ligand (transferrin-conjugated PLGA–PEG) which has enhanced cellular uptake of these nanoparticles in the brain tissues in rat (A. Jain, Chasoo, Singh, Saxena, & Jain, 2011). There are currently eight polymeric micelle-based formulations that include anticancer drugs within them which are in clinical trials (Gong, Chen, Zheng, Wang, & Wang, 2012; Lu & Park, 2013).

One of the most common GBM models for the *in vivo* studies is the mouse model which can recapitulate physiological hallmarks of human glioma pathology. There are 4 general strategies for generation of the mouse models of GBM, as summarized in **Table 4**. In a study by Petrul et al., human xenografted tumors in mice were treated with CA IX antibody-drug conjugate (BAY 79-4620) which showed complete shrinkage of the tumor in some mice even following a single dose (Petrul et al., 2012).

Model	strategies
Xenografts	Subcutaneous or intracranial transplantation of human primary tumor tissue or cell lines into immune deficient or immunocompromised mice
Conventional GEMMs	Pronuclear microinjection of transgenes directly into fertilized oocytes Gene targeting by electroporation of ES cells
Conditional GEMMs	Bacterial Cre-LoxP recombinase system Yeast Flp/FRT inducible system
Viral vectors	Somatic gene transfer using adenovirus- or lentivirus-driven transduction

Table 6. Approaches to mouse models of GBM.

GEMM stands for genetically engineered mouse model. Adapted from (Janbazian, Karamchandani, & Das, 2014) with permission from Elsevier.

Despite the diversity of the animal models used to test the effectiveness of CA IX inhibitors, most of the results show attenuation of tumor growth or a decrease in tumor size (Ditte et al., 2014; Lou et al., 2011) (**Table 6**).

4.7. Modes and Molecular Mechanisms of Cell Death induced by AZT and TMZ

One of the main goals of therapeutic interventions in oncology is to bring the cancer cells to the point-of-no-return with the minimal side effects. Seminal studies by Kreomer and Galluzzi provide detailed accounts of morphological, biochemical and pathophysiological changes in the cells undergoing cell death. These studies summarize the modes of cell death and methodological approaches to study them (Galluzzi, Maiuri, et al., 2007; Kroemer et al., 2009; Kroemer & Perfettini, 2014; Maiuri & Kroemer, 2015)

Apoptosis refers to a 'programmed cell death' which is a major form of cell death and occurs in several steps: initiation and commitment followed by an execution phase (Elmore, 2007). Major characteristics of the apoptosis are rounding-up of the cells, reduction in cellular and nuclear volume (pyknosis), cellular fragmentation (karyorrhexis), and plasma membrane blebbing. Apoptosis can be either mediated through mitochondria (intrinsic pathway) or mediated through death receptor (extrinsic pathway). In both intrinsic and extrinsic apoptotic pathways, caspases which are cyteine proteases can be activated leading to degradation of cell constituents followed by cell death. However, in the extrinsic pathway, an extracellular death ligand (such as FasL) is required to bind to the transmembrane death receptors which in turn leads to activation of caspase-8, then caspase-3 and 7 followed by cell death (Taylor, Cullen, & Martin, 2008). In the intrinsic pathway, variety of stimuli can provoke stress or cell damage leading to activation of BH3-only protein family. Once the activation of BH3 passes a certain threshold, it promotes the assembly of BAX-BAK oligomers in the mitochondrial outer membrane (**Figure 13**). As a result, cytochrome c is released which leads to

formation of apoptosomes followed by activation of caspase-9, caspase-3 and 7 and cell death (Taylor et al., 2008).

Having seen the substantial cell death caused by combined treatment with ATZ and TMZ in both GBM monolayers (under hypoxia) and spheroids (**Figure 8B** and **11B**), we wanted to determine if apoptosis and necrosis are the modes of cell death in GBM under these conditions. We detected picnotic nuclei indicative of apoptotic cell death (**Figure 12A**). We then measured caspase-3 to see if this apoptotic cell death is caspase-3 dependent. We measured caspase-3 activity of the U251N monolayers and spheroids after 6 days treatment with ATZ, TMZ and their combination using a fluorescent based assay (**Figure 12B** and **12C**). Caspase-3 activity was significantly enhanced upon 6 days combined treatment with ATZ and TMZ. It is worth noting that the increase in caspase-3 activity with the combined treatment in comparison with the untreated controls was significantly higher in the monolayers relative to the spheroids likely due to two main reasons: drug penetration is less efficient in spheroids, and cells in spheroids are more antiapoptotic relative to the cells in monolayer cultures (Imamura et al., 2015). Consistent with previous findings described by Imamura et al., the activation of the caspase-3 with the same treatments in the 2D models are generally higher than in the 3D models (Imamura et al., 2015). Caspase-3 is now an established biomarker of apoptosis and necessary for the acquisition of the apoptotic morphology. However, the presence of proteolytically active caspases or the product of their substrates is not sufficient to define apoptosis (Kroemer & Martin, 2005; Kumar, 2007; Lamkanfi, Festjens, Declercq, Vanden Berghe, & Vandenabeele, 2007). Thus as a follow-up experiment, we examined the level of BAX expression after treatment of U251N spheroids with ATZ and TMZ for 6 days (**Figure 13B**). BAX is a pro-apoptotic member of Bcl-2 family. During apoptosis, BAX is translocated from the cytosol to the mitochondrial outer membrane (OM). Then it forms an oligomeric complex which is responsible for formation of a pore on the mitochondrial OM followed by release of pro-apoptotic factors such as cytochrome c and cell death (**Figure 13A**) (Dewson & Kluck, 2009). The most significant BAX expression was observed for ATZ and TMZ combination treatment (1.8 ± 0.5, $p<0.05$).

Taken together, the BAX overexpression and enhanced caspase-3 activity suggests that apoptosis is one of the major mechanisms of cell death caused by ATZ and TMZ treatment in the GBM cell models. Consistent with our results, in a previous study by Arabinda et al., it was shown that the ATZ and TMZ combined treatment caused the most significant enhancement in apoptosis (assessed by ApopTag assay) in T98G and U87MG GBM cell lines compared to the individual treatments (Das et al., 2008).

In addition to apoptosis, there are several other cell death mechanisms which may be responsible for the total cell death caused by ATZ and TMZ combined treatment. Some of the major cell death mechanisms with their characteristics and methods of detection are listed in the **Table 7**.

Cell death mode	**Morphological features**	**Biochemical features**	**Methods of detection (Galluzzi, Zamzami, et al., 2007; Golstein & Kroemer, 2007; Tasdemir et al., 2008)**
Apoptosis	Rounding-up of the cell, Retraction of pseudopods, Reduction of cellular and nuclear, volume (pyknosis), Nuclear fragmentation (karyorrhexis), Minor modification of cytoplasmic organelles, Plasma membrane blebbing, Engulfment by resident phagocytes *in vivo*	Activation and expression of proapoptotic Bcl-2 family proteins (e.g., Bax, Bak, Bid) Activation of caspases Plasma membrane rupture	IF microscopy localization studies, Immunoblotting Colorimetric/fluorogenic substrate-based assays in live cells FACS quantification with vital dyes

Autophagy	Lack of chromatin condensation Massive vacuolization of the cytoplasm, Accumulation of (double-membraned) autophagic vacuoles, Little or no uptake by phagocytic cells *in vivo*	Beclin-1 dissociation from Bcl-2/XL Dependency on atg gene products	Co-immunoprecipitation studies Plasmid-driven overexpression systems
Necrosis	Cytoplasmic swelling (oncosis), Rupture of plasma membrane, Swelling of cytoplasmic, organelles, Moderate chromatin condensation	Drop of ATP levels Activation of calpains	Luminometric assessments of ATP/ADP ratio Colorimetric/fluorogenic substrate-based assays of cell lysates in microtiter plates

Table 7. Distinct modalities of cell death.

Adapted from (Kroemer et al., 2009) with permission from Elsevier.

Necrosis is another major form of cell death. It is accompanied by rapid permeabilization of the plasma membrane, cytoplasmic swelling, and moderate chromatin condensation (Proskuryakov, Konoplyannikov, & Gabai, 2003). One of the main fluorescent dyes, an intercalating agent, which is used for discrimination between apoptosis and necrosis is PI. The healthy plasma membrane is impermeable to PI. During necrosis, there is a rapid permeabilization of the plasma membrane allowing the PI molecules to enter the cells and bind to the nucleic acids (DNA and RNA) in the cells followed by 20-30 fold enhancement in the fluorescent intensity (Proskuryakov et al., 2003).

Following the treatments with ATZ and TMZ, we added PI to the cells. We observed a significant increase in the PI positive cells after 6 days of combined treatment with ATZ

and TMZ suggesting that necrosis may be one of the major mechanisms of cell death under these condition (results, **Figure 8A**).

Conclusions

Overall, the results from this thesis highlight several important findings with regards to the effect of CA IX inhibition in three different GBM model systems:

1) In the U251N monolayers, the simplest GBM model, CA IX was highly induced in a dose dependent manner upon their exposure to $CoCl_2$. Although inhibition of CA IX in the monolayers by ATZ did not significantly enhance cell death, the combined ATZ and TMZ treatment did enhance cell death moderately but significantly in both normoxic and hypoxic conditions.
2) In the U251N spheroids and several types of BTSCs, hypoxia occurred intrinsically (in the core) which led to a time and size dependent increase in CA IX expression. Inhibition of CA IX by ATZ combined with TMZ treatment significantly enhanced cell death after 6 days.
3) The mechanisms of cell death caused by ATZ and TMZ treatment involved significant enhancement of caspase-3 activity and BAX expression which are established biomarkers of apoptosis in the U251N cells, suggesting that apoptosis may be one of the major mechanisms of cell death caused by this treatment.
4) The expression of CA IX in different BTSCs which play a key role in recurrence of GBM, is significantly higher in these cells (up to 6 fold) than in the U251N spheroids. These findings suggest that CA IX could be an interesting target for the drug delivery and elimination of BTSCs.
5) Encapsulation of ATZ into polymeric micelles led to a significant cell death in both U251N and BTSC spheroids. This finding is relevant from the clinical stand point for GBM chemotherapy and other approaches to eradicate GBM.

References

Abuchowski, A., McCoy, J. R., Palczuk, N. C., van Es, T., & Davis, F. F. (1977). Effect of covalent attachment of polyethylene glycol on immunogenicity and circulating life of bovine liver catalase. *J Biol Chem, 252*(11), 3582-3586.

Aggarwal, M., Kondeti, B., & McKenna, R. (2013). Insights towards sulfonamide drug specificity in alpha-carbonic anhydrases. *Bioorg Med Chem, 21*(6), 1526-1533. doi: 10.1016/j.bmc.2012.08.019

Ahlskog, J. K., Dumelin, C. E., Trussel, S., Marlind, J., & Neri, D. (2009). In vivo targeting of tumor-associated carbonic anhydrases using acetazolamide derivatives. *Bioorg Med Chem Lett, 19*(16), 4851-4856. doi: 10.1016/j.bmcl.2009.06.022

Alterio, V., Hilvo, M., Di Fiore, A., Supuran, C. T., Pan, P., Parkkila, S., . . . De Simone, G. (2009). Crystal structure of the catalytic domain of the tumor-associated human carbonic anhydrase IX. *Proc Natl Acad Sci U S A, 106*(38), 16233-16238. doi: 10.1073/pnas.0908301106

Ameres, S. L., & Zamore, P. D. (2013). Diversifying microRNA sequence and function. *Nat Rev Mol Cell Biol, 14*(8), 475-488. doi: 10.1038/nrm3611

Asthagiri, A. R., Pouratian, N., Sherman, J., Ahmed, G., & Shaffrey, M. E. (2007). Advances in brain tumor surgery. *Neurol Clin, 25*(4), 975-1003, viii-ix. doi: 10.1016/j.ncl.2007.07.006

Auffinger, B., Spencer, D., Pytel, P., Ahmed, A. U., & Lesniak, M. S. (2015). The role of glioma stem cells in chemotherapy resistance and glioblastoma multiforme recurrence. *Expert Rev Neurother*, 1-12. doi: 10.1586/14737175.2015.1051968

Badie, B., & Schartner, J. (2001). Role of microglia in glioma biology. *Microsc Res Tech, 54*(2), 106-113. doi: 10.1002/jemt.1125

Badie, B., & Schartner, J. M. (2000). Flow cytometric characterization of tumor-associated macrophages in experimental gliomas. *Neurosurgery, 46*(4), 957-961; discussion 961-952.

Bailey, K. M., Wojtkowiak, J. W., Hashim, A. I., & Gillies, R. J. (2012). Targeting the metabolic microenvironment of tumors. *Adv Pharmacol, 65*, 63-107. doi: 10.1016/b978-0-12-397927-8.00004-x

Bangham, A. D. (1968). Membrane models with phospholipids. *Prog Biophys Mol Biol, 18*, 29-95.

Bernsen, H. J., Rijken, P. F., Peters, H., Raleigh, J. A., Jeuken, J. W., Wesseling, P., & van der Kogel, A. J. (2000). Hypoxia in a human intracerebral glioma model. *J Neurosurg, 93*(3), 449-454. doi: 10.3171/jns.2000.93.3.0449

Bernstein, J. M., Andrews, T. D., Slevin, N. J., West, C. M., & Homer, J. J. (2015). Prognostic value of hypoxia-associated markers in advanced larynx and hypopharynx squamous cell carcinoma. *Laryngoscope, 125*(1), E8-15. doi: 10.1002/lary.24933

Brahimi-Horn, M. C., Bellot, G., & Pouyssegur, J. (2011). Hypoxia and energetic tumour metabolism. *Curr Opin Genet Dev, 21*(1), 67-72. doi: 10.1016/j.gde.2010.10.006

Bralten, L. B., & French, P. J. (2011). Genetic alterations in glioma. *Cancers (Basel), 3*(1), 1129-1140. doi: 10.3390/cancers3011129

Bussink, J., Kaanders, J. H., Rijken, P. F., Peters, J. P., Hodgkiss, R. J., Marres, H. A., & van der Kogel, A. J. (1999). Vascular architecture and microenvironmental parameters in human squamous cell carcinoma xenografts: effects of carbogen and nicotinamide. *Radiother Oncol, 50*(2), 173-184.

Butovsky, O., Jedrychowski, M. P., Moore, C. S., Cialic, R., Lanser, A. J., Gabriely, G., . . . Weiner, H. L. (2014). Identification of a unique TGF-beta-dependent molecular and functional signature in microglia. *Nat Neurosci, 17*(1), 131-143. doi: 10.1038/nn.3599

Cankovic, M., Nikiforova, M. N., Snuderl, M., Adesina, A. M., Lindeman, N., Wen, P. Y., & Lee, E. Q. (2013). The role of MGMT testing in clinical practice: a report of the association for molecular pathology. *J Mol Diagn, 15*(5), 539-555. doi: 10.1016/j.jmoldx.2013.05.011

Casano, A. M., & Peri, F. (2015). Microglia: multitasking specialists of the brain. *Dev Cell, 32*(4), 469-477. doi: 10.1016/j.devcel.2015.01.018

Chen, J., Rocken, C., Hoffmann, J., Kruger, S., Lendeckel, U., Rocco, A., . . . Ebert, M. P. (2005). Expression of carbonic anhydrase 9 at the invasion front of gastric cancers. *Gut, 54*(7), 920-927. doi: 10.1136/gut.2004.047340

Chi, A. S., & Wen, P. Y. (2007). Inhibiting kinases in malignant gliomas. *Expert Opin Ther Targets, 11*(4), 473-496. doi: 10.1517/14728222.11.4.473

Cianchi, F., Vinci, M. C., Supuran, C. T., Peruzzi, B., De Giuli, P., Fasolis, G., . . . Puccetti, L. (2010). Selective inhibition of carbonic anhydrase IX decreases cell proliferation and induces ceramide-mediated apoptosis in human cancer cells. *J Pharmacol Exp Ther, 334*(3), 710-719. doi: 10.1124/jpet.110.167270

Costantino, L., Gandolfi, F., Tosi, G., Rivasi, F., Vandelli, M. A., & Forni, F. (2005). Peptide-derivatized biodegradable nanoparticles able to cross the blood-brain barrier. *J Control Release, 108*(1), 84-96. doi: 10.1016/j.jconrel.2005.07.013

Cukierman, E., Pankov, R., Stevens, D. R., & Yamada, K. M. (2001). Taking cell-matrix adhesions to the third dimension. *Science, 294*(5547), 1708-1712. doi: 10.1126/science.1064829

Dang, L., White, D. W., Gross, S., Bennett, B. D., Bittinger, M. A., Driggers, E. M., . . . Su, S. M. (2010). Cancer-associated IDH1 mutations produce 2-hydroxyglutarate. *Nature, 465*(7300), 966. doi: 10.1038/nature09132

Das, A., Banik, N. L., & Ray, S. K. (2008). Modulatory effects of acetazolomide and dexamethasone on temozolomide-mediated apoptosis in human glioblastoma T98G and U87MG cells. *Cancer Invest, 26*(4), 352-358. doi: 10.1080/07357900701788080

DeAngelis, L. M. (2009). Anaplastic glioma: how to prognosticate outcome and choose a treatment strategy. [corrected]. *J Clin Oncol, 27*(35), 5861-5862. doi: 10.1200/jco.2009.24.5985

Dewson, G., & Kluck, R. M. (2009). Mechanisms by which Bak and Bax permeabilise mitochondria during apoptosis. *J Cell Sci, 122*(Pt 16), 2801-2808.

Dhanikula, R. S., Argaw, A., Bouchard, J. F., & Hildgen, P. (2008). Methotrexate loaded polyether-copolyester dendrimers for the treatment of gliomas: enhanced efficacy and intratumoral transport capability. *Mol Pharm, 5*(1), 105-116. doi: 10.1021/mp700086j

Ditte, Z., Ditte, P., Labudova, M., Simko, V., Iuliano, F., Zatovicova, M., . . . Pastorek, J. (2014). Carnosine inhibits carbonic anhydrase IX-mediated extracellular acidosis and suppresses growth of HeLa tumor xenografts. *BMC Cancer, 14*, 358. doi: 10.1186/1471-2407-14-358

Dolecek, T. A., Propp, J. M., Stroup, N. E., & Kruchko, C. (2012). CBTRUS statistical report: primary brain and central nervous system tumors diagnosed in the United States in 2005-2009. *Neuro Oncol, 14 Suppl 5*, v1-49. doi: 10.1093/neuonc/nos218

Doyen, J., Parks, S. K., Marcie, S., Pouyssegur, J., & Chiche, J. (2012). Knock-down of hypoxia-induced carbonic anhydrases IX and XII radiosensitizes tumor cells by increasing intracellular acidosis. *Front Oncol, 2*, 199. doi: 10.3389/fonc.2012.00199

Dubois, L., Douma, K., Supuran, C. T., Chiu, R. K., van Zandvoort, M. A., Pastorekova, S., . . . Lambin, P. (2007). Imaging the hypoxia surrogate marker CA IX requires expression and catalytic activity for binding fluorescent sulfonamide inhibitors. *Radiother Oncol, 83*(3), 367-373. doi: 10.1016/j.radonc.2007.04.018

Dubois, L., Peeters, S., Lieuwes, N. G., Geusens, N., Thiry, A., Wigfield, S., . . . Lambin, P. (2011). Specific inhibition of carbonic anhydrase IX activity enhances the in vivo therapeutic effect of tumor irradiation. *Radiother Oncol, 99*(3), 424-431. doi: 10.1016/j.radonc.2011.05.045

Dzieciuch, M., Rissanen, S., Szydlowska, N., Bunker, A., Kumorek, M., Jamroz, D., . . . Kepczynski, M. (2015). PEGylated Liposomes as Carriers of Hydrophobic Porphyrins. *J Phys Chem B*. doi: 10.1021/acs.jpcb.5b01351

Ellingson, B. M., Cloughesy, T. F., Pope, W. B., Zaw, T. M., Phillips, H., Lalezari, S., . . . Lai, A. (2012). Anatomic localization of O6-methylguanine DNA methyltransferase (MGMT) promoter methylated and unmethylated tumors: a radiographic study in 358 de novo human glioblastomas. *Neuroimage, 59*(2), 908-916. doi: 10.1016/j.neuroimage.2011.09.076

Elmore, S. (2007). Apoptosis: a review of programmed cell death. *Toxicologic pathology, 35*(4), 495-516.

Engler, A. J., Sen, S., Sweeney, H. L., & Discher, D. E. (2006). Matrix elasticity directs stem cell lineage specification. *Cell, 126*(4), 677-689. doi: 10.1016/j.cell.2006.06.044

Fiano, V., Trevisan, M., Trevisan, E., Senetta, R., Castiglione, A., Sacerdote, C., . . . Merletti, F. (2014). MGMT promoter methylation in plasma of glioma patients receiving temozolomide. *J Neurooncol, 117*(2), 347-357. doi: 10.1007/s11060-014-1395-4

Fiaschi, T., Giannoni, E., Taddei, M. L., Cirri, P., Marini, A., Pintus, G., . . . Chiarugi, P. (2013). Carbonic anhydrase IX from cancer-associated fibroblasts drives epithelial-mesenchymal transition in prostate carcinoma cells. *Cell Cycle, 12*(11), 1791-1801. doi: 10.4161/cc.24902

Fisher, K. E., Pop, A., Koh, W., Anthis, N. J., Saunders, W. B., & Davis, G. E. (2006). Tumor cell invasion of collagen matrices requires coordinate lipid agonist-induced G-protein and membrane-type matrix metalloproteinase-1-dependent signaling. *Mol Cancer, 5*, 69. doi: 10.1186/1476-4598-5-69

Friedman, H. S., Kerby, T., & Calvert, H. (2000). Temozolomide and treatment of malignant glioma. *Clin Cancer Res, 6*(7), 2585-2597.
Friedman, M. D., Jeevan, D. S., Tobias, M., Murali, R., & Jhanwar-Uniyal, M. (2013). Targeting cancer stem cells in glioblastoma multiforme using mTOR inhibitors and the differentiating agent all-trans retinoic acid. *Oncol Rep, 30*(4), 1645-1650. doi: 10.3892/or.2013.2625
Furnari, F. B., Fenton, T., Bachoo, R. M., Mukasa, A., Stommel, J. M., Stegh, A., . . . Cavenee, W. K. (2007). Malignant astrocytic glioma: genetics, biology, and paths to treatment. *Genes Dev, 21*(21), 2683-2710. doi: 10.1101/gad.1596707
Galarneau, H., Villeneuve, J., Gowing, G., Julien, J. P., & Vallieres, L. (2007). Increased glioma growth in mice depleted of macrophages. *Cancer Research, 67*(18), 8874-8881. doi: 10.1158/0008-5472.can-07-0177
Galluzzi, L., Maiuri, M. C., Vitale, I., Zischka, H., Castedo, M., Zitvogel, L., & Kroemer, G. (2007). Cell death modalities: classification and pathophysiological implications. *Cell Death Differ, 14*(7), 1237-1243. doi: 10.1038/sj.cdd.4402148
Galluzzi, L., Zamzami, N., de La Motte Rouge, T., Lemaire, C., Brenner, C., & Kroemer, G. (2007). Methods for the assessment of mitochondrial membrane permeabilization in apoptosis. *Apoptosis, 12*(5), 803-813. doi: 10.1007/s10495-007-0720-1
Gilkes, D. M., Semenza, G. L., & Wirtz, D. (2014). Hypoxia and the extracellular matrix: drivers of tumour metastasis. *Nat Rev Cancer, 14*(6), 430-439. doi: 10.1038/nrc3726
Gillies, R. J., Robey, I., & Gatenby, R. A. (2008). Causes and consequences of increased glucose metabolism of cancers. *J Nucl Med, 49 Suppl 2*, 24s-42s. doi: 10.2967/jnumed.107.047258
Golstein, P., & Kroemer, G. (2007). Cell death by necrosis: towards a molecular definition. *Trends Biochem Sci, 32*(1), 37-43. doi: 10.1016/j.tibs.2006.11.001
Gong, J., Chen, M., Zheng, Y., Wang, S., & Wang, Y. (2012). Polymeric micelles drug delivery system in oncology. *J Control Release, 159*(3), 312-323. doi: 10.1016/j.jconrel.2011.12.012
Grove, J., Gautheron, P., Plazonnet, B., & Sugrue, M. F. (1988). Ocular distribution studies of the topical carbonic anhydrase inhibitors L-643,799 and L-650,719 and related alkyl prodrugs. *J Ocul Pharmacol, 4*(4), 279-290.
Hartmann, C., Meyer, J., Balss, J., Capper, D., Mueller, W., Christians, A., . . . von Deimling, A. (2009). Type and frequency of IDH1 and IDH2 mutations are related to astrocytic and oligodendroglial differentiation and age: a study of 1,010 diffuse gliomas. *Acta Neuropathol, 118*(4), 469-474. doi: 10.1007/s00401-009-0561-9
Hegi, M. E., Diserens, A. C., Gorlia, T., Hamou, M. F., de Tribolet, N., Weller, M., . . . Stupp, R. (2005). MGMT gene silencing and benefit from temozolomide in glioblastoma. *N Engl J Med, 352*(10), 997-1003. doi: 10.1056/NEJMoa043331
Helmlinger, G., Yuan, F., Dellian, M., & Jain, R. K. (1997). Interstitial pH and pO2 gradients in solid tumors in vivo: high-resolution measurements reveal a lack of correlation. *Nat Med, 3*(2), 177-182.
Hemmati, H. D., Nakano, I., Lazareff, J. A., Masterman-Smith, M., Geschwind, D. H., Bronner-Fraser, M., & Kornblum, H. I. (2003). Cancerous stem cells can arise

from pediatric brain tumors. *Proc Natl Acad Sci U S A, 100*(25), 15178-15183. doi: 10.1073/pnas.2036535100

Hilvo, M., Baranauskiene, L., Salzano, A. M., Scaloni, A., Matulis, D., Innocenti, A., . . . Parkkila, S. (2008). Biochemical characterization of CA IX, one of the most active carbonic anhydrase isozymes. *J Biol Chem, 283*(41), 27799-27809. doi: 10.1074/jbc.M800938200

Hochberg, F. H., & Pruitt, A. (1980). Assumptions in the radiotherapy of glioblastoma. *Neurology, 30*(9), 907-911.

Hockel, M., Schlenger, K., Aral, B., Mitze, M., Schaffer, U., & Vaupel, P. (1996). Association between tumor hypoxia and malignant progression in advanced cancer of the uterine cervix. *Cancer Research, 56*(19), 4509-4515.

Holland, E. C. (2000). Glioblastoma multiforme: the terminator. *Proc Natl Acad Sci U S A, 97*(12), 6242-6244.

Ignatova, T. N., Kukekov, V. G., Laywell, E. D., Suslov, O. N., Vrionis, F. D., & Steindler, D. A. (2002). Human cortical glial tumors contain neural stem-like cells expressing astroglial and neuronal markers in vitro. *Glia, 39*(3), 193-206. doi: 10.1002/glia.10094

Imamura, Y., Mukohara, T., Shimono, Y., Funakoshi, Y., Chayahara, N., Toyoda, M., . . . Minami, H. (2015). Comparison of 2D- and 3D-culture models as drug-testing platforms in breast cancer. *Oncol Rep, 33*(4), 1837-1843. doi: 10.3892/or.2015.3767

Ivanov, S., Liao, S. Y., Ivanova, A., Danilkovitch-Miagkova, A., Tarasova, N., Weirich, G., . . . Stanbridge, E. J. (2001). Expression of hypoxia-inducible cell-surface transmembrane carbonic anhydrases in human cancer. *Am J Pathol, 158*(3), 905-919. doi: 10.1016/s0002-9440(10)64038-2

Jain, A., Chasoo, G., Singh, S. K., Saxena, A. K., & Jain, S. K. (2011). Transferrin-appended PEGylated nanoparticles for temozolomide delivery to brain: in vitro characterisation. *J Microencapsul, 28*(1), 21-28. doi: 10.3109/02652048.2010.522257

Jain, R. K. (1999). Transport of molecules, particles, and cells in solid tumors. *Annu Rev Biomed Eng, 1*, 241-263. doi: 10.1146/annurev.bioeng.1.1.241

Janbazian, L., Karamchandani, J., & Das, S. (2014). Mouse models of glioblastoma: lessons learned and questions to be answered. *J Neurooncol, 118*(1), 1-8. doi: 10.1007/s11060-014-1401-x

Jhanwar-Uniyal, M., Labagnara, M., Friedman, M., Kwasnicki, A., & Murali, R. (2015). Glioblastoma: molecular pathways, stem cells and therapeutic targets. *Cancers (Basel), 7*(2), 538-555. doi: 10.3390/cancers7020538

Jordan, C. T., Guzman, M. L., & Noble, M. (2006). Cancer stem cells. *N Engl J Med, 355*(12), 1253-1261. doi: 10.1056/NEJMra061808

Kaluz, S., Kaluzova, M., Liao, S. Y., Lerman, M., & Stanbridge, E. J. (2009). Transcriptional control of the tumor- and hypoxia-marker carbonic anhydrase 9: A one transcription factor (HIF-1) show? *Biochim Biophys Acta, 1795*(2), 162-172. doi: 10.1016/j.bbcan.2009.01.001

Kaminska, B., Kocyk, M., & Kijewska, M. (2013). TGF beta signaling and its role in glioma pathogenesis. *Adv Exp Med Biol, 986*, 171-187. doi: 10.1007/978-94-007-4719-7_9

Kelly, J. J., Stechishin, O., Chojnacki, A., Lun, X., Sun, B., Senger, D. L., . . . Weiss, S. (2009). Proliferation of human glioblastoma stem cells occurs independently of exogenous mitogens. *Stem Cells, 27*(8), 1722-1733. doi: 10.1002/stem.98

Korshunov, A., Ryzhova, M., Hovestadt, V., Bender, S., Sturm, D., Capper, D., . . . Jones, D. T. (2015). Integrated analysis of pediatric glioblastoma reveals a subset of biologically favorable tumors with associated molecular prognostic markers. *Acta Neuropathol, 129*(5), 669-678. doi: 10.1007/s00401-015-1405-4

Kroemer, G., Galluzzi, L., Vandenabeele, P., Abrams, J., Alnemri, E. S., Baehrecke, E. H., . . . Melino, G. (2009). Classification of cell death: recommendations of the Nomenclature Committee on Cell Death 2009. *Cell Death Differ, 16*(1), 3-11. doi: 10.1038/cdd.2008.150

Kroemer, G., & Martin, S. J. (2005). Caspase-independent cell death. *Nat Med, 11*(7), 725-730. doi: 10.1038/nm1263

Kroemer, G., & Perfettini, J. L. (2014). Entosis, a key player in cancer cell competition. *Cell Res, 24*(11), 1280-1281. doi: 10.1038/cr.2014.133

Kumar, S. (2007). Caspase function in programmed cell death. *Cell Death Differ, 14*(1), 32-43. doi: 10.1038/sj.cdd.4402060

Kuroda, J., Kuratsu, J., Yasunaga, M., Koga, Y., Saito, Y., & Matsumura, Y. (2009). Potent antitumor effect of SN-38-incorporating polymeric micelle, NK012, against malignant glioma. *Int J Cancer, 124*(11), 2505-2511. doi: 10.1002/ijc.24171

Lacroix, M., Abi-Said, D., Fourney, D. R., Gokaslan, Z. L., Shi, W., DeMonte, F., . . . Sawaya, R. (2001). A multivariate analysis of 416 patients with glioblastoma multiforme: prognosis, extent of resection, and survival. *J Neurosurg, 95*(2), 190-198. doi: 10.3171/jns.2001.95.2.0190

Lamkanfi, M., Festjens, N., Declercq, W., Vanden Berghe, T., & Vandenabeele, P. (2007). Caspases in cell survival, proliferation and differentiation. *Cell Death Differ, 14*(1), 44-55. doi: 10.1038/sj.cdd.4402047

Lasic, D. D. (1996). Doxorubicin in sterically stabilized liposomes. *Nature, 380*(6574), 561-562. doi: 10.1038/380561a0

Lavon, I., Refael, M., Zelikovitch, B., Shalom, E., & Siegal, T. (2010). Serum DNA can define tumor-specific genetic and epigenetic markers in gliomas of various grades. *Neuro Oncol, 12*(2), 173-180. doi: 10.1093/neuonc/nop041

Lendahl, U., Lee, K. L., Yang, H., & Poellinger, L. (2009). Generating specificity and diversity in the transcriptional response to hypoxia. *Nat Rev Genet, 10*(12), 821-832. doi: 10.1038/nrg2665

Li, A. J., Zheng, Y. H., Liu, G. D., Liu, W. S., Cao, P. C., & Bu, Z. F. (2015). Efficient delivery of docetaxel for the treatment of brain tumors by cyclic RGD-tagged polymeric micelles. *Mol Med Rep, 11*(4), 3078-3086. doi: 10.3892/mmr.2014.3017

Li, S., Lao, J., Chen, B. P., Li, Y. S., Zhao, Y., Chu, J., . . . Chien, S. (2003). Genomic analysis of smooth muscle cells in 3-dimensional collagen matrix. *Faseb j, 17*(1), 97-99. doi: 10.1096/fj.02-0256fje

Li, Y., Wang, H., Oosterwijk, E., Tu, C., Shiverick, K. T., Silverman, D. N., & Frost, S. C. (2009). Expression and activity of carbonic anhydrase IX is associated with metabolic dysfunction in MDA-MB-231 breast cancer cells. *Cancer Invest, 27*(6), 613-623. doi: 10.1080/07357900802653464

Lock, F. E., McDonald, P. C., Lou, Y., Serrano, I., Chafe, S. C., Ostlund, C., . . . Dedhar, S. (2013). Targeting carbonic anhydrase IX depletes breast cancer stem cells within the hypoxic niche. *Oncogene, 32*(44), 5210-5219. doi: 10.1038/onc.2012.550

Lou, Y., McDonald, P. C., Oloumi, A., Chia, S., Ostlund, C., Ahmadi, A., . . . Dedhar, S. (2011). Targeting tumor hypoxia: suppression of breast tumor growth and metastasis by novel carbonic anhydrase IX inhibitors. *Cancer Research, 71*(9), 3364-3376. doi: 10.1158/0008-5472.can-10-4261

Louis, D. N., Ohgaki, H., Wiestler, O. D., Cavenee, W. K., Burger, P. C., Jouvet, A., . . . Kleihues, P. (2007). The 2007 WHO classification of tumours of the central nervous system. *Acta Neuropathol, 114*(2), 97-109. doi: 10.1007/s00401-007-0243-4

Lu, Y., & Park, K. (2013). Polymeric micelles and alternative nanonized delivery vehicles for poorly soluble drugs. *Int J Pharm, 453*(1), 198-214. doi: 10.1016/j.ijpharm.2012.08.042

Maher, E. A., Furnari, F. B., Bachoo, R. M., Rowitch, D. H., Louis, D. N., Cavenee, W. K., & DePinho, R. A. (2001). Malignant glioma: genetics and biology of a grave matter. *Genes Dev, 15*(11), 1311-1333. doi: 10.1101/gad.891601

Mahon, B. P., Pinard, M. A., & McKenna, R. (2015). Targeting carbonic anhydrase IX activity and expression. *Molecules, 20*(2), 2323-2348. doi: 10.3390/molecules20022323

Maiuri, M. C., & Kroemer, G. (2015). Autophagy in stress and disease. *Cell Death Differ, 22*(3), 365-366. doi: 10.1038/cdd.2014.236

Malmstrom, A., Gronberg, B. H., Marosi, C., Stupp, R., Frappaz, D., Schultz, H., . . . Henriksson, R. (2012). Temozolomide versus standard 6-week radiotherapy versus hypofractionated radiotherapy in patients older than 60 years with glioblastoma: the Nordic randomised, phase 3 trial. *Lancet Oncol, 13*(9), 916-926. doi: 10.1016/s1470-2045(12)70265-6

Matsubara, T., Diresta, G. R., Kakunaga, S., Li, D., & Healey, J. H. (2013). Additive Influence of Extracellular pH, Oxygen Tension, and Pressure on Invasiveness and Survival of Human Osteosarcoma Cells. *Front Oncol, 3*, 199. doi: 10.3389/fonc.2013.00199

McDonald, P. C., Winum, J. Y., Supuran, C. T., & Dedhar, S. (2012). Recent developments in targeting carbonic anhydrase IX for cancer therapeutics. *Oncotarget, 3*(1), 84-97.

Moeker, J., Mahon, B. P., Bornaghi, L. F., Vullo, D., Supuran, C. T., McKenna, R., & Poulsen, S. A. (2014). Structural insights into carbonic anhydrase IX isoform specificity of carbohydrate-based sulfamates. *J Med Chem, 57*(20), 8635-8645. doi: 10.1021/jm5012935

Nikiforova, M. N., & Hamilton, R. L. (2011). Molecular diagnostics of gliomas. *Arch Pathol Lab Med, 135*(5), 558-568. doi: 10.1043/2010-0649-rair.1

O'Brien, L. E., Zegers, M. M., & Mostov, K. E. (2002). Opinion: Building epithelial architecture: insights from three-dimensional culture models. *Nat Rev Mol Cell Biol, 3*(7), 531-537. doi: 10.1038/nrm859

Opavsky, R., Pastorekova, S., Zelnik, V., Gibadulinova, A., Stanbridge, E. J., Zavada, J., . . . Pastorek, J. (1996). Human MN/CA9 gene, a novel member of the

carbonic anhydrase family: structure and exon to protein domain relationships. *Genomics, 33*(3), 480-487.
Pardal, R., Clarke, M. F., & Morrison, S. J. (2003). Applying the principles of stem-cell biology to cancer. *Nat Rev Cancer, 3*(12), 895-902. doi: 10.1038/nrc1232
Parks, S. K., Chiche, J., & Pouyssegur, J. (2011). pH control mechanisms of tumor survival and growth. *J Cell Physiol, 226*(2), 299-308. doi: 10.1002/jcp.22400
Pastorekova, S., Ratcliffe, P. J., & Pastorek, J. (2008). Molecular mechanisms of carbonic anhydrase IX-mediated pH regulation under hypoxia. *BJU Int, 101 Suppl 4*, 8-15. doi: 10.1111/j.1464-410X.2008.07642.x
Pasut, G., & Veronese, F. M. (2012). State of the art in PEGylation: the great versatility achieved after forty years of research. *J Control Release, 161*(2), 461-472. doi: 10.1016/j.jconrel.2011.10.037
Penfield, W. (1925). Microglia and the Process of Phagocytosis in Gliomas. *Am J Pathol, 1*(1), 77-90.15.
Perry, V. H., & Gordon, S. (1988). Macrophages and microglia in the nervous system. *Trends Neurosci, 11*(6), 273-277.
Persano, L., Rampazzo, E., Della Puppa, A., Pistollato, F., & Basso, G. (2011). The three-layer concentric model of glioblastoma: cancer stem cells, microenvironmental regulation, and therapeutic implications. *ScientificWorldJournal, 11*, 1829-1841. doi: 10.1100/2011/736480
Petrul, H. M., Schatz, C. A., Kopitz, C. C., Adnane, L., McCabe, T. J., Trail, P., . . . Tamburini, P. P. (2012). Therapeutic mechanism and efficacy of the antibody-drug conjugate BAY 79-4620 targeting human carbonic anhydrase 9. *Mol Cancer Ther, 11*(2), 340-349. doi: 10.1158/1535-7163.mct-11-0523
Piccirillo, S. G., Combi, R., Cajola, L., Patrizi, A., Redaelli, S., Bentivegna, A., . . . Vescovi, A. L. (2009). Distinct pools of cancer stem-like cells coexist within human glioblastomas and display different tumorigenicity and independent genomic evolution. *Oncogene, 28*(15), 1807-1811. doi: 10.1038/onc.2009.27
Pickering, L. M., & Larkin, J. (2015). Kidney cancer: Carbonic anhydrase IX in resected clear cell RCC. *Nat Rev Urol, 12*(6), 309-310. doi: 10.1038/nrurol.2015.124
Potter, C., & Harris, A. L. (2004). Hypoxia inducible carbonic anhydrase IX, marker of tumour hypoxia, survival pathway and therapy target. *Cell Cycle, 3*(2), 164-167.
Proescholdt, M. A., Mayer, C., Kubitza, M., Schubert, T., Liao, S. Y., Stanbridge, E. J., . . . Merrill, M. J. (2005). Expression of hypoxia-inducible carbonic anhydrases in brain tumors. *Neuro Oncol, 7*(4), 465-475. doi: 10.1215/s1152851705000025
Proescholdt, M. A., Merrill, M. J., Stoerr, E. M., Lohmeier, A., Pohl, F., & Brawanski, A. (2012). Function of carbonic anhydrase IX in glioblastoma multiforme. *Neuro Oncol, 14*(11), 1357-1366. doi: 10.1093/neuonc/nos216
Proskuryakov, S. Y., Konoplyannikov, A. G., & Gabai, V. L. (2003). Necrosis: a specific form of programmed cell death? *Exp Cell Res, 283*(1), 1-16.
Radvak, P., Repic, M., Svastova, E., Takacova, M., Csaderova, L., Strnad, H., . . . Kopacek, J. (2013). Suppression of carbonic anhydrase IX leads to aberrant focal adhesion and decreased invasion of tumor cells. *Oncol Rep, 29*(3), 1147-1153. doi: 10.3892/or.2013.2226

Ransohoff, R. M., & Engelhardt, B. (2012). The anatomical and cellular basis of immune surveillance in the central nervous system. *Nat Rev Immunol, 12*(9), 623-635. doi: 10.1038/nri3265

Rao, S. S., Lannutti, J. J., Viapiano, M. S., Sarkar, A., & Winter, J. O. (2014). Toward 3D biomimetic models to understand the behavior of glioblastoma multiforme cells. *Tissue Eng Part B Rev, 20*(4), 314-327. doi: 10.1089/ten.TEB.2013.0227

Reich, R., Hoffman, A., Veerendhar, A., Maresca, A., Innocenti, A., Supuran, C. T., & Breuer, E. (2012). Carbamoylphosphonates control tumor cell proliferation and dissemination by simultaneously inhibiting carbonic anhydrase IX and matrix metalloproteinase-2. Toward nontoxic chemotherapy targeting tumor microenvironment. *J Med Chem, 55*(17), 7875-7882. doi: 10.1021/jm300981b

Reifenberger, J., Reifenberger, G., Liu, L., James, C. D., Wechsler, W., & Collins, V. P. (1994). Molecular genetic analysis of oligodendroglial tumors shows preferential allelic deletions on 19q and 1p. *Am J Pathol, 145*(5), 1175-1190.

Reya, T., Morrison, S. J., Clarke, M. F., & Weissman, I. L. (2001). Stem cells, cancer, and cancer stem cells. *Nature, 414*(6859), 105-111. doi: 10.1038/35102167

Robertson, N., Potter, C., & Harris, A. L. (2004). Role of carbonic anhydrase IX in human tumor cell growth, survival, and invasion. *Cancer Research, 64*(17), 6160-6165. doi: 10.1158/0008-5472.can-03-2224

Roggendorf, W., Strupp, S., & Paulus, W. (1996). Distribution and characterization of microglia/macrophages in human brain tumors. *Acta Neuropathol, 92*(3), 288-293.

Said, H. M., Hagemann, C., Carta, F., Katzer, A., Polat, B., Staab, A., . . . Supuran, C. T. (2013). Hypoxia induced CA9 inhibitory targeting by two different sulfonamide derivatives including acetazolamide in human glioblastoma. *Bioorg Med Chem, 21*(13), 3949-3957. doi: 10.1016/j.bmc.2013.03.068

Sarkar, S., Doring, A., Zemp, F. J., Silva, C., Lun, X., Wang, X., . . . Yong, V. W. (2013). Therapeutic activation of macrophages and microglia to suppress brain tumor-initiating cells. *Ann Neurosci, 20*(4), 154. doi: 10.5214/ans.0972.7531.200407

Sathornsumetee, S., Reardon, D. A., Desjardins, A., Quinn, J. A., Vredenburgh, J. J., & Rich, J. N. (2007). Molecularly targeted therapy for malignant glioma. *Cancer, 110*(1), 13-24. doi: 10.1002/cncr.22741

Sathornsumetee, S., Rich, J. N., & Reardon, D. A. (2007). Diagnosis and treatment of high-grade astrocytoma

Neurol Clin, 25(4), 1111-1139, x. doi: 10.1016/j.ncl.2007.07.004

Semete, B., Booysen, L., Lemmer, Y., Kalombo, L., Katata, L., Verschoor, J., & Swai, H. S. (2010). In vivo evaluation of the biodistribution and safety of PLGA nanoparticles as drug delivery systems. *Nanomedicine, 6*(5), 662-671. doi: 10.1016/j.nano.2010.02.002

Shin, H. J., Rho, S. B., Jung, D. C., Han, I. O., Oh, E. S., & Kim, J. Y. (2011). Carbonic anhydrase IX (CA9) modulates tumor-associated cell migration and invasion. *J Cell Sci, 124*(Pt 7), 1077-1087. doi: 10.1242/jcs.072207

Shinkai, M., Le, B., Honda, H., Yoshikawa, K., Shimizu, K., Saga, S., . . . Kobayashi, T. (2001). Targeting hyperthermia for renal cell carcinoma using human MN antigen-specific magnetoliposomes. *Jpn J Cancer Res, 92*(10), 1138-1145.

Siegal, T. (2015a). Clinical impact of molecular biomarkers in gliomas. *J Clin Neurosci, 22*(3), 437-444. doi: 10.1016/j.jocn.2014.10.004
Siegal, T. (2015b). Clinical impact of molecular biomarkers in gliomas. *J Clin Neurosci, 22*(3), 437-444. doi: 10.1016/j.jocn.2014.10.004
Singh, S. K., Clarke, I. D., Terasaki, M., Bonn, V. E., Hawkins, C., Squire, J., & Dirks, P. B. (2003). Identification of a cancer stem cell in human brain tumors. *Cancer Research, 63*(18), 5821-5828.
Singh, S. K., Hawkins, C., Clarke, I. D., Squire, J. A., Bayani, J., Hide, T., . . . Dirks, P. B. (2004). Identification of human brain tumour initiating cells. *Nature, 432*(7015), 396-401. doi: 10.1038/nature03128
Sorg, B. S., Hardee, M. E., Agarwal, N., Moeller, B. J., & Dewhirst, M. W. (2008). Spectral imaging facilitates visualization and measurements of unstable and abnormal microvascular oxygen transport in tumors. *J Biomed Opt, 13*(1), 014026. doi: 10.1117/1.2837439
Speicher, M. R., & Carter, N. P. (2005). The new cytogenetics: blurring the boundaries with molecular biology. *Nat Rev Genet, 6*(10), 782-792. doi: 10.1038/nrg1692
Stummer, W., Pichlmeier, U., Meinel, T., Wiestler, O. D., Zanella, F., & Reulen, H. J. (2006). Fluorescence-guided surgery with 5-aminolevulinic acid for resection of malignant glioma: a randomised controlled multicentre phase III trial. *Lancet Oncol, 7*(5), 392-401. doi: 10.1016/s1470-2045(06)70665-9
Stupp, R., Mason, W. P., van den Bent, M. J., Weller, M., Fisher, B., Taphoorn, M. J., . . . Mirimanoff, R. O. (2005). Radiotherapy plus concomitant and adjuvant temozolomide for glioblastoma. *N Engl J Med, 352*(10), 987-996. doi: 10.1056/NEJMoa043330
Suva, M. L., Rheinbay, E., Gillespie, S. M., Patel, A. P., Wakimoto, H., Rabkin, S. D., . . . Bernstein, B. E. (2014). Reconstructing and reprogramming the tumor-propagating potential of glioblastoma stem-like cells. *Cell, 157*(3), 580-594. doi: 10.1016/j.cell.2014.02.030
Svenson, S., & Chauhan, A. S. (2008). Dendrimers for enhanced drug solubilization. *Nanomedicine (Lond), 3*(5), 679-702. doi: 10.2217/17435889.3.5.679
Swietach, P., Hulikova, A., Vaughan-Jones, R. D., & Harris, A. L. (2010). New insights into the physiological role of carbonic anhydrase IX in tumour pH regulation. *Oncogene, 29*(50), 6509-6521. doi: 10.1038/onc.2010.455
Swietach, P., Vaughan-Jones, R. D., & Harris, A. L. (2007). Regulation of tumor pH and the role of carbonic anhydrase 9. *Cancer Metastasis Rev, 26*(2), 299-310. doi: 10.1007/s10555-007-9064-0
Tasdemir, E., Galluzzi, L., Maiuri, M. C., Criollo, A., Vitale, I., Hangen, E., . . . Kroemer, G. (2008). Methods for assessing autophagy and autophagic cell death. *Methods Mol Biol, 445*, 29-76. doi: 10.1007/978-1-59745-157-4_3
Taylor, R. C., Cullen, S. P., & Martin, S. J. (2008). Apoptosis: controlled demolition at the cellular level. *Nat Rev Mol Cell Biol, 9*(3), 231-241. doi: 10.1038/nrm2312
Teppo, S., Sundquist, E., Vered, M., Holappa, H., Parkkisenniemi, J., Rinaldi, T., . . . Nyberg, P. (2013). The hypoxic tumor microenvironment regulates invasion of aggressive oral carcinoma cells. *Exp Cell Res, 319*(4), 376-389. doi: 10.1016/j.yexcr.2012.12.010

Vaupel, P., Mayer, A., & Hockel, M. (2004). Tumor hypoxia and malignant progression. *Methods Enzymol, 381*, 335-354. doi: 10.1016/s0076-6879(04)81023-1

Walker, M. D., Alexander, E., Jr., Hunt, W. E., MacCarty, C. S., Mahaley, M. S., Jr., Mealey, J., Jr., . . . Strike, T. A. (1978). Evaluation of BCNU and/or radiotherapy in the treatment of anaplastic gliomas. A cooperative clinical trial. *J Neurosurg, 49*(3), 333-343. doi: 10.3171/jns.1978.49.3.0333

Watters, J. J., Schartner, J. M., & Badie, B. (2005). Microglia function in brain tumors. *J Neurosci Res, 81*(3), 447-455. doi: 10.1002/jnr.20485

Wen, P. Y., & Kesari, S. (2008). Malignant gliomas in adults. *N Engl J Med, 359*(5), 492-507. doi: 10.1056/NEJMra0708126

Wick, W., Naumann, U., & Weller, M. (2006). Transforming growth factor-beta: a molecular target for the future therapy of glioblastoma. *Curr Pharm Des, 12*(3), 341-349.

Wingo, T., Tu, C., Laipis, P. J., & Silverman, D. N. (2001). The catalytic properties of human carbonic anhydrase IX. *Biochem Biophys Res Commun, 288*(3), 666-669. doi: 10.1006/bbrc.2001.5824

Yamada, K. M., & Cukierman, E. (2007). Modeling tissue morphogenesis and cancer in 3D. *Cell, 130*(4), 601-610. doi: 10.1016/j.cell.2007.08.006

Yi, L., Xiao, H., Xu, M., Ye, X., Hu, J., Li, F., . . . Feng, H. (2011). Glioma-initiating cells: a predominant role in microglia/macrophages tropism to glioma. *J Neuroimmunol, 232*(1-2), 75-82. doi: 10.1016/j.jneuroim.2010.10.011

Yung, W. K., Albright, R. E., Olson, J., Fredericks, R., Fink, K., Prados, M. D., . . . Levin, V. A. (2000). A phase II study of temozolomide vs. procarbazine in patients with glioblastoma multiforme at first relapse. *Br J Cancer, 83*(5), 588-593. doi: 10.1054/bjoc.2000.1316

Zavada, J., Zavadova, Z., Pastorek, J., Biesova, Z., Jezek, J., & Velek, J. (2000). Human tumour-associated cell adhesion protein MN/CA IX: identification of M75 epitope and of the region mediating cell adhesion. *Br J Cancer, 82*(11), 1808-1813. doi: 10.1054/bjoc.2000.1111

Zeppernick, F., Ahmadi, R., Campos, B., Dictus, C., Helmke, B. M., Becker, N., . . . Herold-Mende, C. C. (2008). Stem cell marker CD133 affects clinical outcome in glioma patients. *Clin Cancer Res, 14*(1), 123-129. doi: 10.1158/1078-0432.ccr-07-0932